Article

Not peer-reviewed version

Optimization of Battery Energy Storage Systems for Prosumers and Energy Communities Under Capacity-Based Tariffs

Tomislav Markotić , Matej Žnidarec , Damir Šljivac , Edin Lakić , Danijel Topić *

Posted Date: 23 March 2026

doi: 10.20944/preprints202603.1588.v1

Keywords: battery energy storage systems; techno-economic analysis; optimization; prosumer; energy community; capacity-based network tariffs

 doi:10.20944/preprints202603.1588.v1

Article

Optimization of Battery Energy Storage Systems for Prosumers and Energy Communities Under Capacity-Based Tariffs

Tomislav Markotić [1], Matej Žnidarec [1], Damir Šljivac [1], Edin Lakić [2] and Danijel Topić [1,*]

[1] Faculty of Electrical Engineering, Computer Science and Information Technology Osijek, Josip Juraj Strossmayer University of Osijek, 31000 Osijek, Croatia
[2] Institute for Innovation and Development of University of Ljubljana, 1000 Ljubljana , Slovenia;
* Correspondence: danijel.topic@ferit.hr

Abstract

The transition toward capacity-based network tariffs shifts the primary role of battery energy storage systems (BESS) from traditional energy arbitrage to active peak shaving. This paper presents a mixed-integer linear programming (MILP) optimization model for the co-optimization of both BESS size and operation scheduling for multiple prosumers operating individually and within energy community (EC). The model accounts for battery cyclic degradation and reduces the state of health (SOH) over the project lifetime. The framework is evaluated by a comprehensive techno-economic analysis of BESS integration under Slovenia's multi-block tariff structure. The results demonstrate that while individual distributed BESS integration is highly profitable, centralized EC BESS financially underperforms. Because centralized BESS cannot directly reduce individual contracted power limits, its profitability relies on energy arbitrage, making the initial investment and double grid fees the primary barriers. Conversely, integrating distributed storage with peer-to-peer (P2P) trading minimizes the required BESS capacity while maintaining profitability. The evaluation also reveals that ECs do not automatically act as socio-economic equalizers, indicated by a stable Gini coefficient. However, a break-even analysis reveals the necessary reduction in capital costs to overcome these hurdles, confirming the strong future viability of centralized EC BESS.

Keywords: battery energy storage systems; techno-economic analysis; optimization; prosumer; energy community; capacity-based network tariffs

1. Introduction

The growing integration of renewable energy sources (RES), particularly photovoltaic (PV) systems, into low-voltage (LV) grids has shifted the operational paradigm of distribution systems. This transition towards an active distribution grid is no longer a future scenario but a present operational reality. However, the existing grid infrastructure faces increasing challenges in accommodating further RES hosting capacity. As highlighted by the International Energy Agency (IEA), grid modernization and digitalization are becoming critical prerequisites to prevent infrastructure from acting as a limiting factor in the energy transition [1]. This trend is further supported by the "REPowerEU" plan, which aims to accelerate the deployment of rooftop PV systems across the residential and commercial sectors to enhance energy independence, thereby increasing the operational complexity of LV networks [2].

Consequently, the stochastic nature of RES generation, which often mismatches local consumption profiles, leads to frequent bidirectional power flows [3]. These reverse power flows lead to technical challenges, including voltage deviations, line congestion, transformer overloading, and increased grid losses [3–7]. Beyond these technical constraints, the economic landscape has also evolved. While early PV profitability relied heavily on favorable feed-in tariffs [8], their gradual phase-out under

 doi:10.20944/preprints202603.1588.v1

modern tariff structures has shifted the economic rationale toward maximizing self-consumption and minimizing grid reliance. In this context, battery energy storage systems (BESS) have emerged as a critical solution to mitigate RES intermittency and enhance the operational flexibility of the power system [9,10].

However, the effective deployment of BESS relies heavily on optimal sizing and operation strategies that balance upfront investment costs against long-term operational savings. Consequently, mixed-integer linear programming (MILP) has emerged as the dominant methodological approach due to its robustness in handling complex constraints [11]. In this domain, recent research [12] successfully employed an MILP framework to optimize prosumer operations, demonstrating that BESS integration can simultaneously minimize costs and quantify reductions in distribution grid losses. Despite these advancements, recent studies increasingly emphasize the need to accurately account for BESS's battery wear to prevent overly optimistic profit estimates. In [13], a MILP model for home energy management systems (HEMS) was developed that explicitly integrates cycle-aging factors, such as depth of discharge (DOD). The results indicated that while intensive cycling can reduce short-term energy bills by up to 26.56%, it significantly accelerates degradation, necessitating careful optimization trade-offs. Similarly, a two-stage optimization framework was utilized in [14] to demonstrate that cyclic aging is the dominant cost component, and neglecting it leads to suboptimal capacity sizing. To address these aging mechanisms, [15] applied the Rainflow counting algorithm and validated that BESS can remain profitable even after the standard warranty period, provided that the state of health (SOH) is actively managed. Furthermore, [16] compared MILP against dynamic programming for battery cell revamping strategies, confirming that MILP effectively balances short-term arbitrage against long-term replacement needs. Regarding investment viability in the context of the circular economy, [17] highlighted that detailed degradation modeling is the decisive factor, finding that second-life batteries remain economically infeasible compared to new units due to their rapid health deterioration. While MILP remains the widely adopted method for precise techno-economic sizing, recent reviews in [18] and [19] highlight the growing complexity of coordinating large-scale communities. To address computational challenges in such heterogeneous environments, the study in [20] proposed clustering algorithms to group prosumers with similar consumption patterns prior to optimization. Furthermore, beyond deterministic approaches, game-theoretic models have gained traction for resolving multi-agent conflicts. In [21], evolutionary game theory is applied to model dynamic peer-to-peer (P2P) interactions, while in [22], a novel "rental energy storage" concept governed by Stackelberg games is introduced, offering an alternative to direct ownership. Therefore, to ensure a globally optimal solution while rigorously accounting for BESS battery aging, this paper adopts a MILP framework that explicitly models degradation mechanisms. This approach balances short-term arbitrage gains against preserving the battery's SOH, thereby ensuring a realistic assessment of the system's long-term techno-economic viability.

Beyond optimizing individual units, the comparative economic viability of centralized versus distributed storage systems is a key research priority. Numerous studies have analyzed the economic implications of these opposing structures. In [23], the economic performance of community-level storage was investigated, demonstrating that shared infrastructure significantly reduces net present costs compared to distributed equivalents due to economies of scale. Similarly, [24] highlighted that centralized BESSs enable the simultaneous provision of multiple ancillary services, thereby allowing operators to co-optimize behind-the-meter cost savings with front-of-meter market revenues. Furthermore, [25] showed that a centralized provider model requires less total installed capacity to achieve the same level of service, effectively mitigating the synchronization of peak loads often observed in uncoordinated distributed systems [26].

Conversely, the distributed storage model is favored for its autonomy and resilience, particularly when enabled by P2P trading mechanisms. In [27], it was found that although individual storage systems may have lower base profitability, integrating P2P markets allows prosumers to monetize excess generation more effectively than standard feed-in tariffs, thereby validating private investment.

 doi:10.20944/preprints202603.1588.v1

The study in [28] confirmed this financial shift, showing that local energy trading can significantly reduce the payback period for residential PV-battery systems. From a security perspective, [29] emphasized resilience, noting that although distributed systems may be more capital-intensive, they offer greater reliability during grid outages by maintaining an independent power supply for each household.

In addition to ownership structures, market mechanisms, and regulatory frameworks critically impact the economic viability of BESS. the optimal capacity sizing and operational scheduling of BESS. In [30], a "Battery-as-a-Service" model was proposed, demonstrating that precise price forecasting significantly improves revenue stacking in volatile markets. Moreover, local regulations dictate the operational boundaries of these systems. In the Italian context, studies [31] and [32] developed models specifically to maximize "shared energy" incentives, illustrating how national rules directly shape the technical design and profitability of storage systems.

Given the observed gaps in the literature, this paper presents a comprehensive techno-economic comparison of individual prosumer strategies and community-based BESS solutions. While existing MILP-based optimization studies [12,13] have effectively investigated operational aspects, and others have analyzed specific energy-sharing models [23,28], the literature reveals significant limitations in long-term evaluation horizons. Most current studies rely on short-term simulations, ranging from a single day to a few weeks, and then extrapolate these results over the project lifetime. Furthermore, the economic impact of emerging capacity-based network tariffs remains largely unexplored in this comparative context. As multi-block billing schemes are increasingly implemented, relying solely on energy-only tariffs and short-term operational models no longer captures the true lifetime economic potential of BESS.

To bridge these gaps, this paper introduces a comprehensive techno-economic framework that evaluates BESS integration through an MILP model. The core objective is to determine whether prosumers achieve superior financial outcomes by operating individually or within an energy community (EC), and to evaluate both centralized and distributed BESS configurations. The unique contributions of this paper, highlighted in Table 1, lie in the following methodological advancements:

- **Lifetime co-optimization framework:** Developing a MILP model that simultaneously co-optimizes BESS sizing and operation scheduling over a complete 15-year project lifetime. Unlike standard models that rely on short-term extrapolation of data, this approach dynamically internalizes the costs of cyclic degradation and linear SOH reduction to prevent long-term profit overestimation.
- **Advanced tariff integration:** Explicitly incorporating complex multi-block capacity-based network tariffs into the mathematical objective function. By distinguishing between volumetric energy (kWh) and contracted power (kW) charges, the model captures the operational shift from traditional energy arbitrage to active peak shaving.
- **Evaluation of energy sharing architectures:** Developing distinct mathematical formulations to represent and evaluate various operational setups, including isolated prosumers, centralized BESS (C-BESS), and distributed BESS (D-BESS) integrated with P2P energy trading. This unified framework enables a quantitative comparison of their techno-economic performance while incorporating the Gini coefficient as a post-optimization metric to explicitly evaluate the socio-economic fairness of financial distribution among participants.

 doi:10.20944/preprints202603.1588.v1

Table 1. Comparative overview of the proposed framework against selected state-of-the-art techno-economic studies.

Reference	Optimization scope	Tariff framework	Evaluated configurations	Degradation modeling	Evaluation horizon
[12]	Operation	Energy (Time of Use)	Individual	None	1-Year (extrapolated)
[13]	Operation	Energy (Time of Use)	Individual	Cycle aging	1-Day
[23]	Sizing & operation	Energy only	Individual + C-BESS + P2P	Simplified (O&M)	4 Weeks (extrapolated)
[28]	Operation	Dynamic / Spot	Individual + P2P	Fixed assumption	2 Weeks (extrapolated)
Proposed	**Sizing & operation**	**Energy + capacity**	**Individual + C-BESS + P2P**	**Cyclic cost + SOH**	**15-Year**

The remainder of this paper is organized as follows. Section 1 introduces the research context, reviews the relevant literature, and defines the specific research gaps and contributions. Section 2 details the proposed methodology, including the mathematical formulation of the MILP model and the integration of the capacity-based network tariff structure. Section 3 presents the case study by defining the input data, the observed operational scenarios, and the computational results. Section 4 provides a critical discussion of the findings, focusing on the comparative techno-economic viability of the scenarios and on the sensitivity and break-even assessments. Finally, section 5 summarizes the main conclusions of the study.

2. Methodology

The methodological framework developed in this study provides a comprehensive techno-economic evaluation of BESS integration across different prosumer ownership structures, assessing their financial viability relative to a baseline scenario in which prosumers operate with PV systems only. The primary objective of the proposed approach is to simultaneously co-optimize the BESS capacity and its operational scheduling to minimize the total cost of ownership (TCO) over the entire BESS lifetime. The core of the framework is structured around an MILP model. MILP was selected for its proven robustness and computational efficiency in solving complex energy management problems with discrete decision variables, making it well-suited for extensive, multi-year techno-economic assessments [18].

To ensure scalability and broad applicability, the mathematical model is formulated using a flexible set of parameters and decision variables. This modular design allows the framework to evaluate and compare distinct operational configurations, ranging from individual prosumer setups to centralized community storage and distributed P2P structures. A critical aspect integrated into this framework is the explicit modeling of a complex capacity-based network tariff. This tariff structure accounts for both active energy consumption and contracted peak power across diverse seasonal blocks, and is coupled with an internalized, linearized battery degradation mechanism to prevent unrealistic profit estimations. Furthermore, to efficiently assess the economic feasibility of the BESS investment, the optimization algorithm determines the optimal capacity and scheduling for a representative base year. These optimized profiles are then incorporated into a multi-year simulation loop that dynamically adjusts for annual battery degradation and economic inflation. The structure of the proposed methodological framework, covering the entire process from input data collection to the final sensitivity analysis, is illustrated in Figure 1.

 doi:10.20944/preprints202603.1588.v1

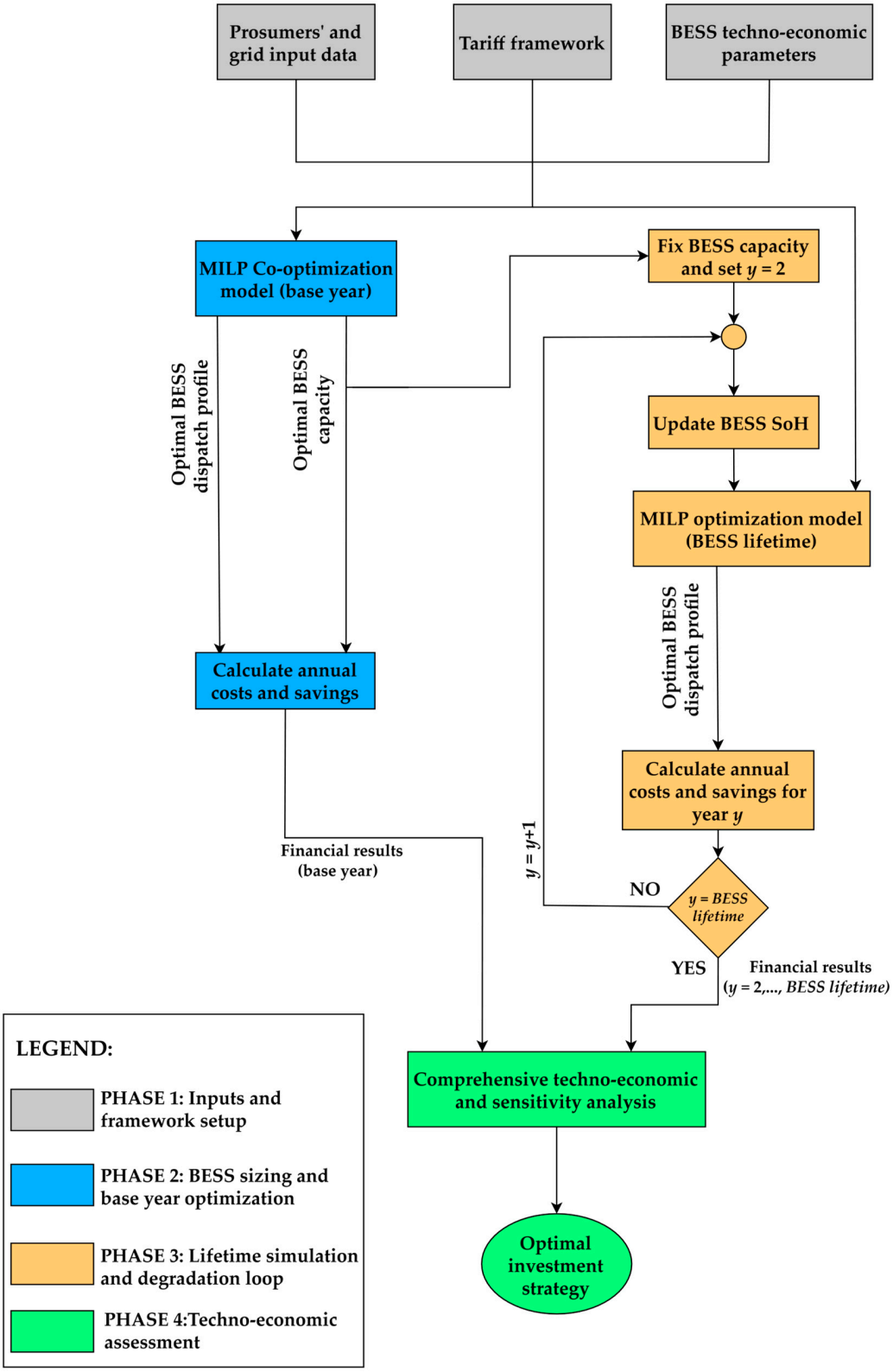

Figure 1. Flowchart of the proposed methodological framework.

The proposed methodological framework comprises four distinct stages, as illustrated in Figure 1. The process begins with Phase 1 (grey): Inputs and framework setup. In this phase, high-resolution time-series data (15-minute resolution) are collected, specifically load profiles and PV generation profiles. Additionally, the technical parameters of the BESS and the specific constraints of capacity-based tariff are defined. These inputs form the basis for Phase 2 (blue): Sizing and base year optimization.

 doi:10.20944/preprints202603.1588.v1

At this stage, the MILP algorithm determines the optimal BESS capacity and operational dispatch for the representative base year ($y = 1$) to minimize the TCO. The resulting optimal capacity is then fixed and serves as an input for Phase 3 (orange): Lifetime simulation and degradation loop. Unlike static approaches, this phase iteratively re-optimizes the BESS dispatch for each year of the BESS lifetime. This loop dynamically accounts for battery aging through a linear SOH degradation mechanism and adjusts for economic factors such as inflation. Finally, the aggregated annual net cash flows from the entire operation period are consolidated in Phase 4 (green): Techno-economic assessment. In this final stage, the project's viability is evaluated using cumulative financial metrics such as net present value (NPV) to identify the optimal investment strategy.

The core optimization model is formulated as an MILP problem. In the primary sizing stage, the central objective is to minimize the total annualized cost of the analyzed system configuration, explicitly accounting for both investment annuities and operating expenses (OPEX), across the scenarios defined in section 3.2. Conversely, during the lifetime simulation, the model minimizes solely the annual operational costs. Both computational stages strictly adhere to a set of technical and regulatory constraints. These include the power balance equations, which ensure that generation and BESS discharge meet consumption requirements at each 15-minute interval, as well as BESS technical limits that define the charging and discharging power, state-of-charge (SOC) boundaries, and cycle degradation costs. Furthermore, the model incorporates grid and tariff constraints that restrict power exchange based on connection power limits and enforce the specific rules of the capacity-based network charge. Consequently, the framework is applicable to diverse investment strategies, from standalone prosumers to ECs with P2P trading, without altering the underlying mathematical formulation.

2.1. Formulation of the Objective Function and Operational Costs

The proposed economic model establishes a universal methodological framework for accurately evaluating the financial performance of prosumer and EC configurations. The model is adaptable to capacity-based network tariff structures that are increasingly being adopted globally to mitigate grid congestion. To ensure universality, the mathematical formulation is defined for a generalized set of system users and time intervals. Let H denote the set of households indexed by h, T the set of time intervals indexed by t, M the set of monthly billing periods indexed by m, and B the set of time blocks indexed by b. The framework formulates operational costs based on bi-directional volumetric energy exchange, contracted peak-power capacity, local trading fees (applicable to both P2P trading and community BESS utilization), constraint-violation penalties, and BESS investment and degradation.

Following a two-stage computational approach, the objective function differs between the sizing phase and the operational lifetime simulation. As defined in the framework overview, the primary goal is to minimize the TCO over the entire BESS lifetime. To achieve this in the primary sizing stage (base year, $y = 1$), the universal objective function is formulated to minimize the equivalent annualized total cost (C^h_{total}), representing the annualized TCO for each household h, as defined in (1):

$$\min C^h_{\text{total}} = C^h_{\text{vol}} + C^h_{\text{cap}} + C^h_{\text{local}} - I^h_{\text{PV}} - I^h_{\text{local}} + C^h_{\text{deg}} + C^h_{\text{pen}} + C^h_{\text{inv,ann}}, \ \forall h \in H \tag{1}$$

Conversely, during the lifetime simulation loop, the model sequentially evaluates each operational year $y \in \{2, \ldots, L_{\text{proj}}\}$, where L_{proj} corresponds to the BESS lifetime. In this phase, the initially sized BESS capacity is fixed, treating the BESS investment as a sunk cost. Consequently, the sequential objective function reduces to minimizing the OPEX costs (C^h_{OPEX}) for each specific year y, defined in (2) as:

$$\min C^h_{\text{OPEX}}(y) = C^h_{\text{vol}}(y) + C^h_{\text{cap}}(y) + C^h_{\text{local}}(y) - I^h_{\text{PV}}(y) - I^h_{\text{local}}(y) + C^h_{\text{deg}}(y) + C^h_{\text{pen}}(y), \ \forall h \in H \tag{2}$$

where: C^h_{vol} is the total volumetric cost for energy import; C^h_{cap} is the capacity charge for contracted peak power; C^h_{local} represents the total cost incurred from importing energy through the local P2P network, encompassing both the agreed internal market price and the specific network charges; I^h_{PV} is the revenue from surplus PV export to the grid; I^h_{local} is the revenue from P2P energy trading; C^h_{pen}

 doi:10.20944/preprints202603.1588.v1

represents the mathematical shadow penalties ensuring strict grid constraint adherence; C^h_{deg} is the total annual battery degradation cost; and $C^h_{\text{inv,ann}}$ is the annualized BESS investment cost.

The fundamental components of the volumetric cost and PV revenue are calculated discretely across the entire set of time intervals $t \in T$, as defined in (3) and (4):

$$C^h_{\text{vol}} = \Delta t \cdot \sum_{t=1}^{T} P^h_{\text{imp}}(t) \cdot c_{\text{vol}}(t), \ \forall h \in H \tag{3}$$

$$I^h_{\text{PV}} = \Delta t \cdot \sum_{t=1}^{T} P^h_{\text{exp}}(t) \cdot c_{\text{exp}}(t), \ \forall h \in H \tag{4}$$

where: t is the time index; T is the total number of time intervals in the observed period; $P^h_{\text{imp}}(t)$ and $P^h_{\text{exp}}(t)$ are the power imported from and exported to the grid by household h, respectively; $c_{\text{vol}}(t)$ is the generic unit volumetric price for imported electricity; $c_{\text{exp}}(t)$ is the unit grid export price; and Δt is the time step duration.

To ensure universal applicability across diverse national policies, the unit volumetric price of electricity imported from the grid, $c_{\text{vol}}(t)$, is disaggregated into several underlying components. For every interval t, it is defined in (5) as:

$$c_{\text{vol}}(t) = c_{\text{market}}(t) + c_{\text{trans,vol}}(t) + c_{\text{dist,vol}}(t) + c_{\text{tax}}(t), \ \forall t \in T \tag{5}$$

where: $c_{\text{market}}(t)$ is the unit retail electricity price provided by the supplier; $c_{\text{trans,vol}}(t)$ is the unit volumetric network fee for energy transmission; $c_{\text{dist,vol}}(t)$ is the unit volumetric network fee for energy distribution; and $c_{\text{tax}}(t)$ represents applicable unit fixed taxes and excise duties.

Calculated on a per-billing-period basis, the aggregate capacity-based network fee C^h_{cap} is formulated to account for multi-block network tariffs globally, defined in (6) as:

$$C^h_{\text{cap}} = \sum_{m=1}^{M} \sum_{b=1}^{B} P^h_{\text{con}}(m,b) \cdot c_{\text{cap}}(m,b), \ \forall h \in H \tag{6}$$

where: m is the billing period index; M is the total number of billing periods in a year; b is the time block index; B is the total number of blocks; $P^h_{\text{con}}(m,b)$ is the optimized contracted peak power of household h for billing period m and time block b; and $c_{\text{cap}}(m,b)$ is the specific aggregate capacity tariff applicable to that block.

Similarly to the volumetric energy price, the unit aggregate capacity tariff $c_{\text{cap}}(m,b)$, applied per billing period, is disaggregated into several underlying components, as defined in (7):

$$c_{\text{cap}}(m,b) = c_{\text{trans,cap}}(m,b) + c_{\text{dist,cap}}(m,b) + c_{\text{RES}}(m,b), \ \forall m \in M, \forall b \in B \tag{7}$$

where: $c_{\text{trans,cap}}(m,b)$ is the unit capacity fee for energy transmission; $c_{\text{dist,cap}}(m,b)$ is the unit capacity fee for energy distribution; and $c_{\text{RES}}(m,b)$ is the unit RES incentive fee applied per kW of contracted power in each respective time block.

In EC configurations, local P2P trading introduces specific financial interactions. The total cost incurred from importing shared energy (C^h_{local}) comprises both the agreed internal market price paid to the exporting peer and the specific local grid utilization fee paid to the distribution system operator. Conversely, exporting surplus energy within the community generates direct peer revenue (I^h_{local}). These are defined in equations (8) and (9):

 doi:10.20944/preprints202603.1588.v1

$$C^h_{\text{local}} = \Delta t \cdot \sum_{t=1}^{T} \left(c_{\text{local,market}}(t) + c_{\text{dist,vol}}(t)\right) \cdot P^h_{\text{local,imp}}(t),\ \forall h \in H \tag{8}$$

$$I^h_{\text{local}} = \Delta t \cdot \sum_{t=1}^{T} P^h_{\text{local,exp}}(t) \cdot c_{\text{local,market}}(t),\ \forall h \in H \tag{9}$$

where: $P^h_{\text{local,imp}}(t)$ and $P^h_{\text{local,exp}}(t)$ are the power imported and exported locally within the EC by household h, respectively and $c_{\text{local,market}}(t)$ is the agreed unit internal market price for P2P transactions.

To ensure a fair and equitable distribution of financial benefits among the EC members, the internal P2P market price is modeled using the standard split-the-difference pricing mechanism. This establishes the internal energy price as the exact arithmetic mean of the unit retail electricity price (c_{market}) and the unit grid export price (c_{exp}), as defined in (10):

$$c_{\text{local,market}}(t) = \frac{c_{\text{market}}(t) + c_{\text{exp}}(t)}{2},\ \forall t \in T \tag{10}$$

To maintain strict adherence to grid connection limits and contracted power boundaries, the shadow penalty C^h_{pen} acts as a rigid mathematical constraint ensuring grid stability, as defined in (11):

$$C^h_{\text{pen}} = \sum_{t=1}^{T} P^h_{\text{exc}}(t) \cdot c_{\text{penalty}},\ \forall h \in H \tag{11}$$

where: $P^h_{\text{exc}}(t)$ is the excess power dynamically exceeding the optimally contracted block limit at any interval t for household h; and c_{penalty} is a sufficiently large, constant penalty coefficient.

Rather than serving as a regulatory billing mechanism, this coefficient functions purely as a soft-constraint penalty, mathematically forcing the solver to strictly prevent capacity violations.

The investment ($C^h_{\text{inv,ann}}$) and degradation (C^h_{deg}) costs, critical for preventing unrealistic energy arbitrage and ensuring accurate BESS sizing, are formulated using the capital recovery factor (CRF), as defined in (12), (13), and (14):

$$C^h_{\text{inv,ann}} = c_{\text{BESS}} \cdot E^h_{\text{nom}} \cdot CRF,\ \forall h \in H \tag{12}$$

$$CRF = \frac{r(1+r)^{L_{\text{proj}}}}{(1+r)^{L_{\text{proj}}} - 1} \tag{13}$$

$$C^h_{\text{deg}} = c_{\text{deg}} \cdot \Delta t \cdot \sum_{t=1}^{T} P^h_{\text{dis}}(t),\ \forall h \in H \tag{14}$$

where: c_{BESS} is the specific capital expenditure of the BESS; E^h_{nom} is the decision variable representing the nominal BESS capacity of household h; r is the discount rate; L_{proj} is the project lifetime (equivalent to the total BESS lifetime); $P^h_{\text{dis}}(t)$ is the BESS discharging power of household h; C^h_{deg} is the annual battery degradation cost; and c_{deg} is the specific unit degradation cost applied per kWh of discharged energy.

By integrating C^h_{deg} directly into the objective function, the solver is mathematically constrained from performing aggressive, low-margin energy arbitrage that would prematurely degrade the battery.

2.2. Modeling of System Components, Technical Constraints and Performance Indicators

The proposed optimization framework is defined by specific physical and technical constraints that establish the system's operational boundaries. These constraints are categorized into three main groups: the technical limits of the PV system, the dynamic characteristics of the BESS, and the grid

 doi:10.20944/preprints202603.1588.v1

interaction rules. The model simultaneously optimizes the installed capacity and the operational schedule, ensuring that the power balance equations and maximum allowable export limits are strictly respected at every time step t.

2.2.1. PV System Sizing

The installed capacity of the PV system is determined based on the specific energy requirements of each prosumer, aiming to achieve a balanced self-sufficiency potential. For each household h, the nominal installed power ($P^h_{\text{PV,nom}}$) is calculated as the ratio of the household's total annual electricity consumption to the specific PV electricity generation potential of the location, as defined in (15):

$$P^h_{\text{PV,nom}} = \frac{E^h_{\text{load,annual}}}{Y_{\text{spec}}}, \ \forall h \in H \tag{15}$$

where: $E^h_{\text{load,annual}}$ is the total annual electricity consumption of household h (kWh); and Y_{spec} is the specific annual PV generation yield characteristic of the geographical location (kWh/kWp) and $P^h_{\text{PV,nom}}$ is the resulting nominal installed PV power (kWp).

2.2.2. Battery Energy Storage System modeling and Constraints

While the following mathematical constraints are formulated using the household index h to represent D-BESS configurations, identical operational logic and physical limitations apply to the C-BESS. For the C-BESS, the index h is omitted, and the variables govern the single aggregated unit.

The BESS is modeled as a controllable storage unit with discrete sizing. The nominal BESS capacity ($E^h_{\text{nom},0}$) for each user h is defined in (16):

$$E^h_{\text{nom},0} = N^h_{\text{bat}} \cdot \Delta E_{\text{block}}, \ \forall h \in H \tag{16}$$

where N^h_{bat} is the integer decision variable representing the number of installed battery blocks; and ΔE_{block} is the specific capacity increment per block. This discrete formulation ensures that the model selects commercially available battery capacities rather than unrealistic continuous fractional values.

Battery aging is modeled through the state of health (SOH), which decreases linearly over the project lifetime based on the annual degradation factor (δ_{deg}), as expressed in (17):

$$SOH(y) = 1 - [(y-1) \cdot \delta_{\text{deg}}], \ \forall y \in Y \tag{17}$$

where: $SOH(y)$ is the state of health factor in year y, expressed as a dimensionless value; and δ_{deg} is the annual degradation factor, defined as a dimensionless factor per year ($year^{-1}$) (e.g., 0.02 for a 2% annual capacity loss).

Consequently, the available nominal BESS capacity ($E^h_{\text{nom}}(y)$) for any given operational year y is reduced relative to the initially installed capacity, as defined in (18):

$$E^h_{\text{nom}}(y) = E^h_{\text{nom},0} \cdot SOH(y), \ \forall h \in H, \forall y \in Y \tag{18}$$

where: $E^h_{\text{nom}}(y)$ represents the usable capacity of the BESS in year y.

The simulation for each year begins with an initial state of energy ($E^h_{\text{bat}}(0)$), derived from the specific capacity of that year and the initial state of charge (SOC_{init}), as defined in (19):

$$E^h_{\text{bat}}(0) = E^h_{\text{nom}}(y) \cdot SOC_{\text{init}}, \ \forall h \in H \tag{19}$$

 doi:10.20944/preprints202603.1588.v1

The state of energy (E^h_{bat}) is calculated for each time step t based on the previous timestep $(t-1)$, formulated in (20):

$$E^h_{\text{bat}}(t) = E^h_{\text{bat}}(t-1) + \left(P^h_{\text{ch}}(t) \cdot \eta_{\text{ch}} - \frac{P^h_{\text{dis}}(t)}{\eta_{\text{dis}}} \right) \cdot \Delta t, \ \forall h \in H, \forall t \in T \tag{20}$$

where: $P^h_{\text{ch}}(t)$ and $P^h_{\text{dis}}(t)$ are the BESS charging and discharging powers at time t, respectively; and $\eta_{\text{ch}}, \eta_{\text{dis}}$ are the charging and discharging efficiencies of the BESS.

Simultaneous charging and discharging of the BESS is naturally prevented by the optimization logic; such behavior would strictly incur energy losses due to conversion inefficiencies and trigger unnecessary degradation penalties within the objective function, making it economically suboptimal.

The (SOC^h) is defined in (21) as:

$$SOC^h(t) = \frac{E^h_{\text{bat}}(t)}{E^h_{\text{nom}}(y)}, \ \forall h \in H, \forall t \in T \tag{21}$$

BESS SOC is limited between minimum (SOC_{min}) and maximum (SOC_{max}) value, as expressed in (22):

$$SOC_{\text{min}} \leq SOC^h(t) \leq SOC_{\text{max}}, \ \forall h \in H, \forall t \in T \tag{22}$$

To ensure cyclic consistency for the simulation year, the final SOC is strictly constrained to match the pre-defined target value (SOC_{final}), defined in (23) as:

$$SOC^h(T) = SOC_{\text{final}} \quad , \forall h \in H \tag{23}$$

The BESS charging and discharging power limits are governed by the C-rate applied to the available nominal BESS capacity, expressed in (24) and (25):

$$0 \leq P^h_{\text{ch}}(t) \leq C_{\text{rate}} \cdot E^h_{\text{nom}}(y), \ \forall h \in H, \forall t \in T \tag{24}$$

$$0 \leq P^h_{\text{dis}}(t) \leq C_{\text{rate}} \cdot E^h_{\text{nom}}(y), \ \forall h \in H, \forall t \in T \tag{25}$$

where C_{rate} is the nominal maximum C-rate specified by the battery manufacturer, representing the maximum allowable power-to-energy ratio for safe charging and discharging operations.

2.2.3. Power balance and grid interaction constraints

The fundamental constraint in the model is the power balance, which ensures energy conservation in each time interval t. This implies that the total consumption and power outflows must be equal to the total generation and power inflows. The mathematical formulation of this constraint, applicable to both individual prosumers and EC members, is defined in (26):

$$P^h_{\text{load}}(t) + P^h_{\text{ch}}(t) + P^h_{\text{exp}}(t) + P^h_{\text{local,exp}}(t) + P^h_{\text{curt}}(t) = P^h_{\text{PV}}(t) + P^h_{\text{dis}}(t) + P^h_{\text{imp}}(t) + P^h_{\text{local,imp}}(t), \ \forall h \in H, \forall t \in T \tag{26}$$

where: $P^h_{\text{load}}(t)$ represents the household load at timestep t; $P^h_{\text{PV}}(t)$ is the available PV generation at time step t; and $P^h_{\text{curt}}(t)$ is the curtailed PV power at time step t. The curtailment variable is introduced to provide operational flexibility and ensure mathematical feasibility within the solver. Specifically, it enables the system to curtail excess PV generation during periods of high PV generation

 doi:10.20944/preprints202603.1588.v1

when the BESS is fully charged, the local load is satisfied, and the maximum grid export limits are reached, thereby maintaining grid compliance.

The interaction with the distribution grid is limited by the connection capacity (P^h_{conn}). For individual prosumers not participating in an EC, the local exchange variables ($P^h_{\text{local,imp}}(t)$ and $P^h_{\text{local,exp}}(t)$) are strictly set to zero. The total imported power is constrained by the full connection rating, while the total exported power to the grid is limited by a specific regulatory factor (k_{exp}), as defined in (27) and (28):

$$P^h_{\text{imp}}(t) + P^h_{\text{local,imp}}(t) \leq P^h_{\text{conn}}, \ \forall h \in H, \forall t \in T \tag{27}$$

$$P^h_{\text{exp}}(t) + P^h_{\text{local,exp}}(t) \leq k_{\text{exp}} \cdot P^h_{\text{conn}}, \ \forall h \in H, \forall t \in T \tag{28}$$

where: P^h_{conn} is the connection power limit; and k_{exp} is the export limitation coefficient.

The contracted power (P^h_{con}) is optimized for each billing period m and time block b, within the allowable technical range, as defined in (29):

$$P^h_{\text{con,min}} \leq P^h_{\text{con}}(m,b) \leq P^h_{\text{conn}}, \ \forall h \in H, \forall m \in M, \forall b \in B \tag{29}$$

where: $P^h_{\text{con,min}}$ is the administrative minimum contracted power, determined based on the connection capacity.

Furthermore, capacity-based tariff frameworks often dictate a strict nesting rule for contracted power across time blocks. The capacity contracted in a lower-cost block must be greater than or equal to the capacity contracted in the preceding, more expensive block. This mathematical restriction is formulated in (30):

$$P^h_{\text{con}}(m,b) \leq P^h_{\text{con}}(m,b+1), \ \forall h \in H, \forall m \in M, \forall b \in \{1,\ldots,B-1\} \tag{30}$$

The excess power (P^h_{exc}) exceeding the contracted capacity is calculated to quantify penalty costs. Since penalties apply only to positive deviations, this is modeled using two inequalities, as defined in (31) and (32):

$$P^h_{\text{exc}}(t) \geq P^h_{\text{imp}}(t) - P^h_{\text{con}}(m,b), \ \forall h \in H, \forall t \in T \tag{31}$$

$$P^h_{\text{exc}}(t) \geq 0, \ \forall h \in H, \forall t \in T \tag{32}$$

2.3. Comprehensive tEchno-Economic Analysis Model and Performance Metrics

To quantify the operational efficiency and financial viability of the analyzed investment strategies, a comprehensive techno-economic analysis model was developed. This model integrates technical efficiency metrics with long-term financial indicators to enable a robust comparison across diverse system topologies, explicitly distinguishing between individual prosumer strategies and collaborative EC models with either distributed or centralized BESS.

2.3.1. Technical performance metrics

The degree of energy independence and the local utilization efficiency are quantified using the self-sufficiency rate (SSR) and the self-consumption rate (SCR). The fundamental variable in these calculations is the directly utilized PV generation (E^h_{utilized}), defined as the portion of PV generation

 doi:10.20944/preprints202603.1588.v1

used to cover the load or charge the BESS, excluding grid exports and curtailment. This is calculated in (33) as:

$$E^h_{\text{utilized}} = \Delta t \cdot \sum_{t=1}^{T} \left(P^h_{\text{PV}}(t) - P^h_{\text{exp}}(t) - P^h_{\text{local,exp}}(t) - P^h_{\text{curt}}(t) \right), \ \forall h \in H \tag{33}$$

Consequently, the SSR and SCR are defined in (34) and (35):

$$SSR^h = \frac{E^h_{\text{utilized}}}{E^h_{\text{load,annual}}} \cdot 100, \ \forall h \in H \tag{34}$$

$$SCR^h = \frac{E^h_{\text{utilized}}}{E^h_{\text{PV,annual}}} \cdot 100, \ \forall h \in H \tag{35}$$

where: $E^h_{\text{load,annual}}$ and $E^h_{\text{PV,annual}}$ represent the total annual electricity demand and potential PV generation of household h.

Given the focus on capacity-based tariffs, the model uses the power cost share (ζ^h_{power}) to quantify the impact of peak-load management. This metric represents the proportion of the total electricity bill attributed solely to contracted power charges, defined in (36). While primarily calculated annually, this metric is also evaluated monthly to assess the seasonal impacts of tariffs.

$$\zeta^h_{\text{power}} = \frac{C^h_{\text{cap,annual}}}{C^h_{\text{bill,total}}} \cdot 100, \ \forall h \in H \tag{36}$$

where: $C^h_{\text{cap,annual}}$ is the total annual cost of contracted power capacity; and $C^h_{\text{bill,total}}$ is the total gross annual electricity bill, including all levies and taxes.

2.3.2. Community Cost Allocation Mechanism

In scenarios with a centralized community BESS, the optimization model minimizes the EC's aggregate TCO. However, to evaluate individual financial performance, these centralized costs must be fairly distributed post-optimization.

The capital investment of the shared BESS ($C_{\text{inv,comm}}$) is allocated proportionally based on the nominal installed PV capacity ($P_{\text{PV,nom}}$) of each household. This approach ensures that the assigned share of storage investment corresponds directly to the individual renewable generation potential, as defined in (37):

$$C^h_{\text{inv}} = C_{\text{inv,comm}} \cdot \frac{P^h_{\text{PV,nom}}}{\sum_{i=1}^{H} P^i_{\text{PV,nom}}}, \ \forall h \in H \tag{37}$$

where: C^h_{inv} is the allocated total investment cost for household h; $C_{\text{inv,comm}}$ is the total investment cost of the central BESS; and $P^h_{\text{PV,nom}}$ is the nominal installed PV capacity of household h.

Conversely, the OPEX generated directly by the centralized BESS functioning as a distinct grid entity (such as its own grid import, charging fees, and contracted peak power charges) are distributed volumetrically. Each household pays a dynamic share proportional to the total energy discharged from the central BESS to the respective household, as defined in (38):

$$C^h_{\text{OPEX,comm}} = C_{\text{OPEX,total}} \cdot \frac{\Delta t \cdot \sum_{t=1}^{T} P^h_{\text{from\_bess}}(t)}{\Delta t \cdot \sum_{i=1}^{H} \sum_{t=1}^{T} P^i_{\text{from\_bess}}(t)}, \ \forall h \in H \tag{38}$$

where: $C^h_{\text{OPEX,comm}}$ is the allocated OPEX of the central BESS for household h; $C_{\text{OPEX,total}}$ is the total annual operational bill of the central BESS unit; and $P^h_{\text{from\_bess}}(t)$ is the discharged power from the central BESS to household h at time interval t.

 doi:10.20944/preprints202603.1588.v1

In centralized community storage scenarios, the shared BESS capacity ($E^{\text{comm}}_{\text{bat}}$) is virtually allocated to individual members to determine their respective shares of investment costs and benefits. The allocation key is defined proportionally to the installed PV capacity of each prosumer, as formulated in (39):

$$E^{h}_{\text{bat,alloc}} = E^{\text{comm}}_{\text{bat}} \cdot \frac{P^{h}_{\text{PV,nom}}}{\sum_{i=1}^{H} P^{i}_{\text{PV,nom}}}, \ \forall h \in H \tag{39}$$

where: $E^{h}_{\text{bat,alloc}}$ is the allocated BESS capacity for household h; and $E^{\text{comm}}_{\text{bat}}$ represents the total installed capacity of the centralized community BESS.

2.3.3. Financial Viability Analysis And Distributional Fairness

As previously defined in the section 2.1, a degradation cost penalty (C^{h}_{deg}) is included within the MILP objective function to prevent unrealistic battery micro-cycling. However, it must be emphasized that this strictly serves as an operational soft penalty. To avoid double-counting, this specific cost component is excluded from the ex-post financial evaluation. Instead, the true economic impact of battery aging is accounted for through the physical reduction in SOH over the project lifetime and the eventual end-of-life decommissioning costs.

Although excluded from the MILP objective to maintain linearity and solver efficiency, fixed constants, such as monthly metering fees and value-added tax (VAT), are fully accounted for in the post-optimization techno-economic assessment. The final gross household bill is calculated as defined in (40):

$$C^{h}_{\text{bill,gross}} = (C^{h}_{\text{vol}} + C^{h}_{\text{cap}} + C^{h}_{\text{local}} - I^{h}_{\text{PV}} - I^{h}_{\text{local}} + C_{\text{fixed}} + C^{h}_{\text{OPEX,comm}}) \cdot (1 + \text{VAT}), \ \forall h \in H \tag{40}$$

where: C_{fixed} represents the total annual fixed supplier fee per metering point; and $C^{h}_{\text{OPEX,comm}}$ represents the prosumer's allocated share of the shared community battery's energy-related operational costs (e.g., costs incurred from grid electricity imports). To clearly distinguish between the operational architectures, this parameter applies exclusively to the centralized C-BESS scenarios, whereas for individual distributed configurations (D-BESS), it is strictly set to zero.

To systematically quantify the economic viability of the proposed BESS integrations relative to a baseline scenario (PV-only), the annual net cost savings (ANC) metrics are utilized. Adapted from the methodology proposed in [12], the absolute (ANC^{h}_{abs}) and percentage (ANC^{h}_{perc}) savings for each household h are defined in (41) and (42):

$$ANC^{h}_{\text{abs}} = C^{h,\text{ref}}_{\text{bill,gross}} - C^{h,\text{eval}}_{\text{bill,gross}}, \ \forall h \in H \tag{41}$$

$$ANC^{h}_{\text{perc}} = \left(\frac{C^{h,\text{ref}}_{\text{bill,gross}} - C^{h,\text{eval}}_{\text{bill,gross}}}{C^{h,\text{ref}}_{\text{bill,gross}} } \right) \cdot 100, \ \forall h \in H \tag{42}$$

where: $C^{h,\text{ref}}_{\text{bill,gross}}$ represents the total gross annual bill of household h in the Baseline reference scenario (PV systems only); and $C^{h,\text{eval}}_{\text{bill,gross}}$ represents the total gross annual bill in the evaluated BESS integration scenario (denoted by the superscript "eval").

Long-term economic performance is evaluated using the net present value (NPV), return on investment (ROI), and the discounted payback period (PBP). The analysis spans the BESS lifetime (L_{proj}), explicitly accounting for the initial capital expenditures (CAPEX) (C^{h}_{inv}), annual operation and maintenance costs ($C^{h}_{\text{O\&M}}$) and the end-of-life decommissioning costs (C^{h}_{decomm}).

The primary metric for this analysis is the annual net cash flow ($CF^{h}(y)$), calculated for each year y as defined in (43):

 doi:10.20944/preprints202603.1588.v1

$$CF^h(y) = ANC^h(y) - C^h_{\text{O\&M}}(y),\ \forall y \in [1, L_{\text{proj}}] \tag{43}$$

where: $ANC^h(y)$ represents the annual net cost savings. This variable captures the inflation-adjusted difference between the baseline and optimized scenario bills, accounting for the annual increase in energy prices and BESS degradation effects, and $C^h_{\text{O\&M}}(y)$ denotes the annual operation and maintenance cost.

Consequently, the (NPV) is calculated by discounting annual cash flows to the base year, as expressed in (44):

$$NPV^h = -C^h_{\text{inv}} - \frac{C^h_{\text{decomm}}}{(1+r)^{L_{\text{proj}}}} + \sum_{y=1}^{L_{\text{proj}}} \frac{CF^h(y)}{(1+r)^y},\ \forall h \in H \tag{44}$$

ROI measures profitability relative to capital cost. It is derived as the ratio of the NPV to the initial investment, calculated according to (45):

$$ROI^h = \frac{NPV^h}{C^h_{\text{inv}}} \cdot 100,\ \forall h \in H \tag{45}$$

PBP is determined by tracking the cumulative discounted cash flow (CCF^h). It is defined as the year Y where CCF^h transitions from negative to positive, indicating that the initial investment has been fully recovered. CCF^h is calculated as defined in (46):

$$CCF^h(Y) = -C^h_{\text{inv}} + \sum_{y=1}^{Y} \frac{CF^h(y)}{(1+r)^y},\ \forall h \in H, \forall Y \in [1, L_{\text{proj}}] \tag{46}$$

Finally, for scenarios involving ECs, the fairness of the benefit distribution is assessed using the Gini coefficient (G). This indicator is computed based on the distribution of the achieved NPVs across the EC members, as expressed in:

$$G = \frac{\sum_{i=1}^{N} \sum_{j=1}^{N} |NPV^i - NPV^j|}{2 \cdot N \cdot \sum_{i=1}^{N} NPV^i} \tag{47}$$

where: N is the total number of EC members; and NPV^i and NPV^j represent the net present values of EC members i and j. A coefficient of 0 indicates perfect equality, while a value closer to 1 implies significant disparity in the achieved financial benefits.

3. Results

In this section, the results obtained by applying the methodology described in the section 2 are presented and analyzed in detail. It begins by presenting the main input data based on real-world measurements from the Luče, Slovenia case study, along with the specific tariff configuration settings used in the models. Subsequently, the system's performance is evaluated at the prosumer level, accounting for optimized operating profiles and economic savings. Furthermore, the comparative economic viability of centralized versus distributed BESS configurations is analyzed, including distributional fairness. Finally, the cumulative results of the targeted sensitivity analysis regarding investment costs and energy price variations are presented.

 doi:10.20944/preprints202603.1588.v1

3.1. Input Data

This subsection systematically presents all essential input data used to parametrize the optimization models and conduct comprehensive techno-economic and distributional fairness analyses. The inputs are categorized into technical system parameters, covering prosumers' load profiles, PV generation data, and BESS specifications, and into economic parameters, comprising the specific capacity-based tariff structure and the BESS investment and operating costs.

3.1.1. Prosumers' Operation Profiles and BESS Parameters

The case study analyzes 15 households in Luče, Slovenia. To ensure the validity of the simulation results, the study uses high-resolution verified measurement load data. The physical load and generation profiles correspond to the reference year 2021. This selection is justified by the availability of a complete, validated 15-minute-resolution dataset, which ensures that the temporal correlation between demand peaks and PV generation is strictly preserved.

The load profiles were obtained from smart meters installed at the prosumers' premises. To obtain realistic renewable generation patterns, the specific PV power output time-series were extracted from the PVGIS online tool [33]. The data was generated using the PVGIS-SARAH 3 solar radiation database, assuming standard crystalline silicon (c-Si) PV technology with optimized slope and azimuth angles. Since the raw dataset provides hourly PV generation values normalized to 1 kWp, a pre-processing step involving time-based linear interpolation was applied to downscale the profiles to a matching 15-minute resolution. The resulting specific annual PV generation for the analyzed location was determined to be 1148.92 kWh/kWp.

The key technical parameters of the 15 analyzed households are summarized in Table 2. The connection power limits (P^h_{conn}) were determined according to the standard connection capacity values defined in [34]. Furthermore, to ensure grid stability and compliance with local technical requirements, the maximum permissible export power into the grid is constrained to 80% of the connection capacity ($k_{\text{exp}} = 0.8$). Additionally, according to the methodology for calculating network charges [35], a minimum limit for P^h_{con} is applied to satisfy the constraint in equation (29). This lower bound ($P^h_{\text{con,min}}$) is set to 31% of the connection capacity for single-phase users (min. 1.8 kW) and 20% for three-phase users (min. 2.8 kW).

Table 2. Annual load, grid connection, and PV system characteristics of the analyzed prosumers.

Prosumer ID	$E^h_{\text{load,annual}}$ (kWh)	P^h_{conn} (kW)	$E^h_{\text{PV,annual}}$ (kWh)	$P^h_{\text{PV,nom}}$ (kWp)
H01	5750.95	11.00	5744.58	5.00
H02	10,717.08	14.00	10,340.25	9.00
H03	5100.94	11.00	5744.58	5.00
H04	8834.94	14.00	9191.33	8.00
H05	6506.39	11.00	6893.50	6.00
H06	8210.89	14.00	8042.42	7.00
H07	3256.64	8.00	3446.75	3.00
H08	3818.32	7.00	3446.75	3.00
H09	8769.31	14.00	9191.33	8.00
H10	4540.46	7.00	4595.67	4.00
H11	6352.38	11.00	6893.50	6.00
H12	8888.26	14.00	9191.33	8.00
H13	11,699.11	14.00	11,489.17	10.00
H14	3748.85	7.00	3446.75	3.00
H15	7201.40	11.00	6893.50	6.00

While Table 2 summarizes the annual energy totals, the simulation requires high-resolution data to capture the mismatch between load and PV generation. Figure 2 depicts the load and PV generation for a representative prosumer (H01) during two specific periods: a typical winter week characterized

 doi:10.20944/preprints202603.1588.v1

by high consumption, and a summer week dominated by excess PV generation. To provide a complete annual perspective, Figure 3 shows the load and PV generation intensity over the year. In these heatmaps, the horizontal axis represents the months, while the vertical axis shows the time of day, enabling clear identification of peak load periods and the daily PV generation profiles.

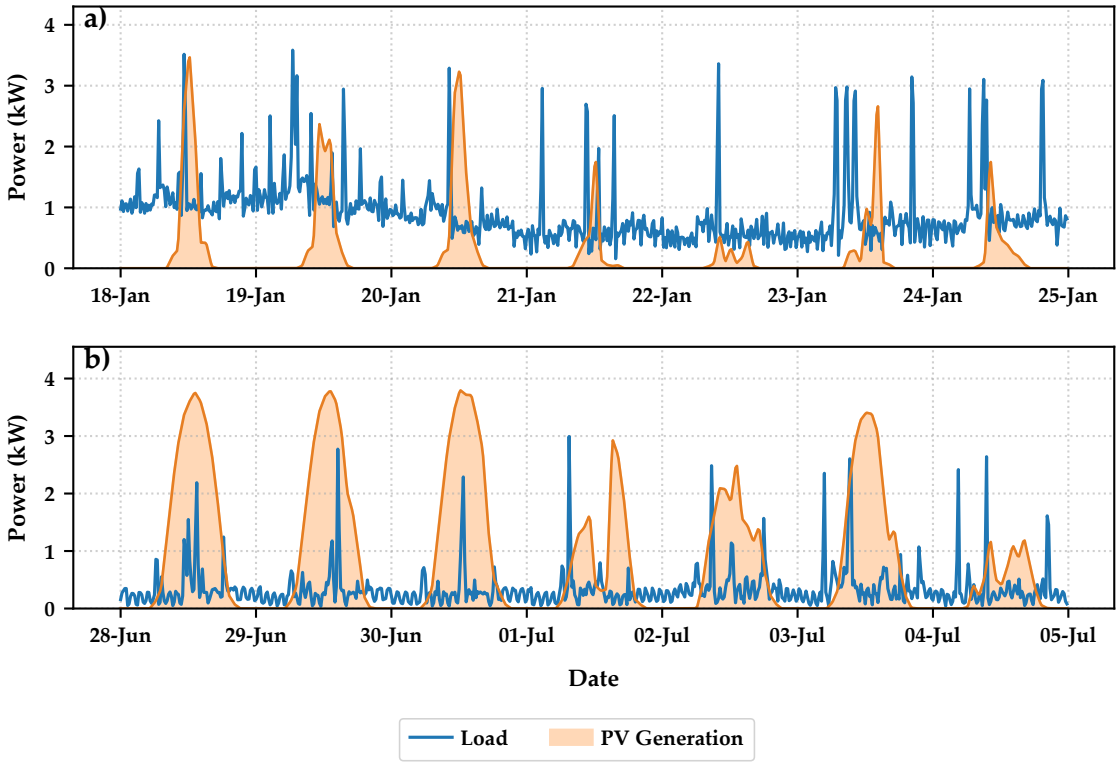

Figure 2. Load and PV generation profiles for a representative prosumer (H01). (**a**) Representative winter week; (**b**) Representative summer week.

 doi:10.20944/preprints202603.1588.v1

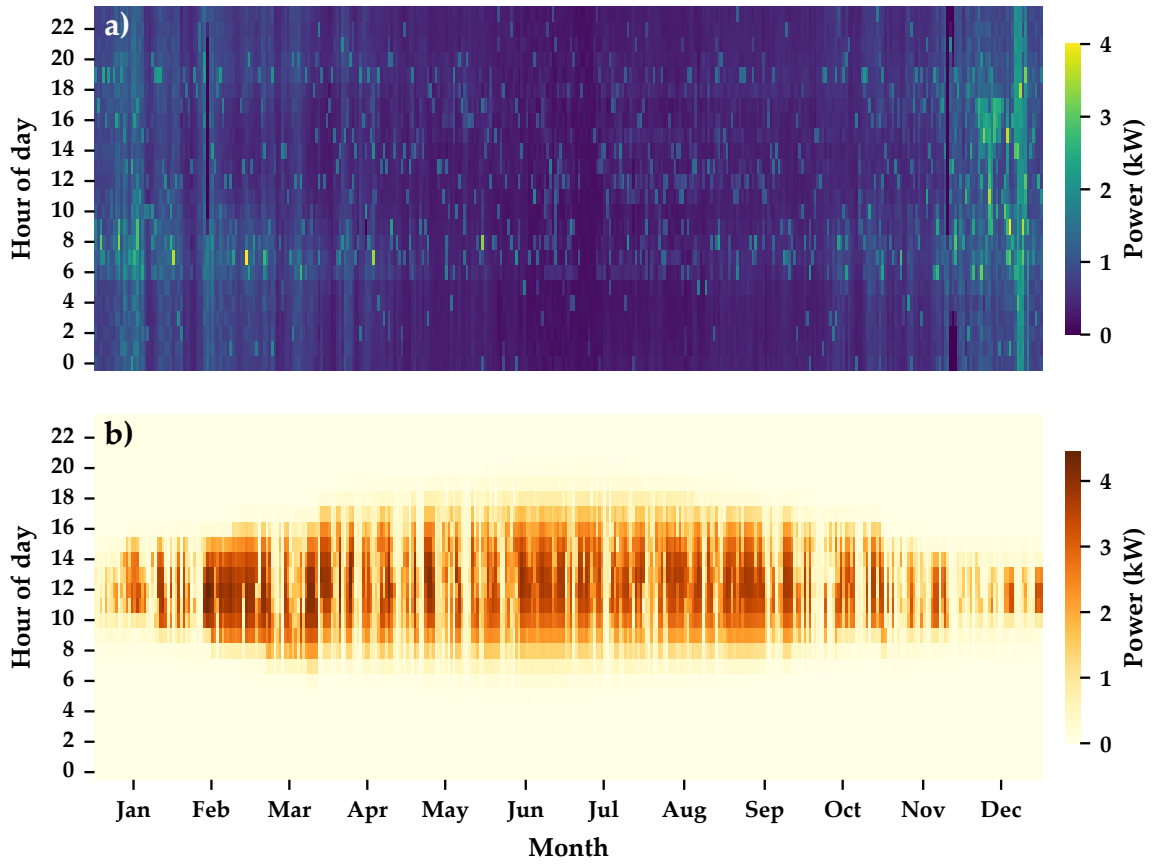

Figure 3. Annual load and PV generation heatmaps for a representative prosumer (H01). (**a**) Annual load profile; (**b**) Annual PV generation profile.

For this paper, the selected 15 prosumers are modeled as connected to a representative low-voltage radial feeder. This topological representation visualizes the physical placement of the BESS units and distinguishes between the storage-integration concepts used in the different simulation scenarios. Figure 4 illustrates the system layout. The diagram clearly defines the two approaches: C-BESS, highlighted by the blue frame, is active in scenarios 2 and 3, while D-BESS, marked with green frames, is utilized in scenarios 1 and 4.

 doi:10.20944/preprints202603.1588.v1

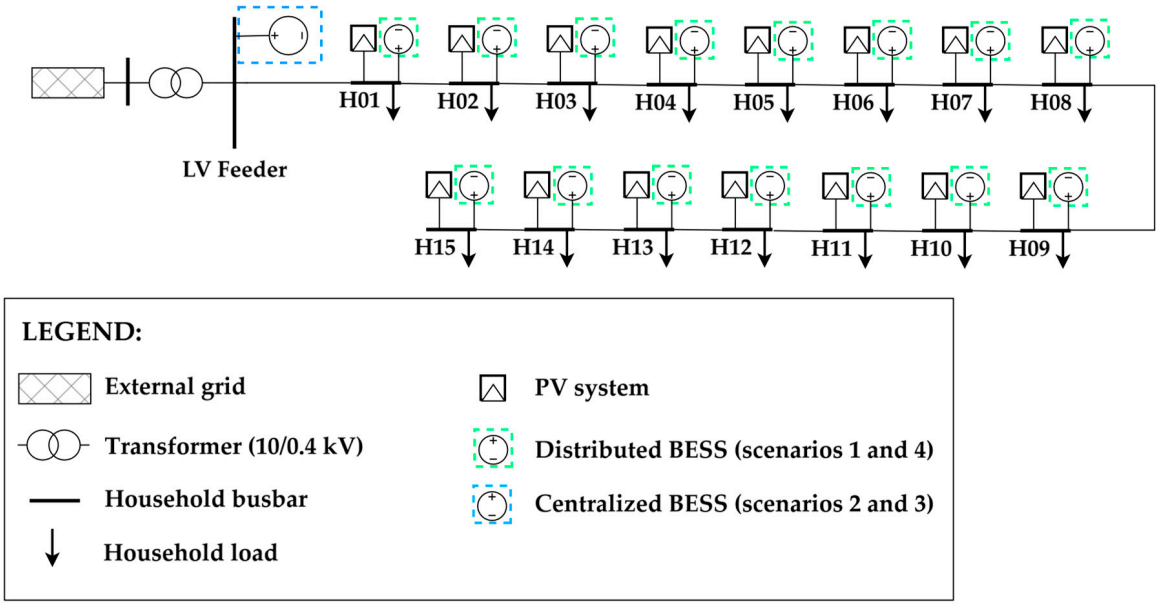

Figure 4. Single line diagram of the modeled LV feeder in Luče, Slovenia.

Table 3. Technical parameters of the modeled BESS.

Parameter	Symbol	Value	Unit
Charging efficiency	η_{ch}	0.95	–
Discharging efficiency	η_{dis}	0.95	–
Maximum C-rate	C_{rate}	0.50	h^{-1}
Capacity sizing step	ΔE_{block}	0.50	kWh
Minimum SOC	SOC_{min}	0.20	–
Maximum SOC	SOC_{max}	1.00	–
DOD	DOD	0.80	–
Initial SOC	SOC_{init}	0.50	–
Target end SOC	SOC_{final}	0.20	–
Annual degradation factor	δ_{deg}	0.02	$year^{-1}$
Project lifetime	L_{proj}	15.00	years

3.1.2. Economic Parameters and the Slovenian Tariff Framework

The economic viability of the proposed system configurations is evaluated under the current Slovenian regulatory framework [35–37]. This tariff system represents a shift from traditional energy-based billing towards a capacity-based structure, designed to reflect the true cost of grid utilization and incentivize peak shaving.

The pricing scheme follows a complex time-of-use (ToU) structure. The year is divided into two seasons: the high season (HS) and the low season (LS). During these seasons, network charges are billed in five time blocks (B1–B5) [35]. B1 denotes critical peak hours with the highest cost, whereas B5 denotes off-peak periods. The time distribution of these blocks is visualized in Figure 5.

 doi:10.20944/preprints202603.1588.v1

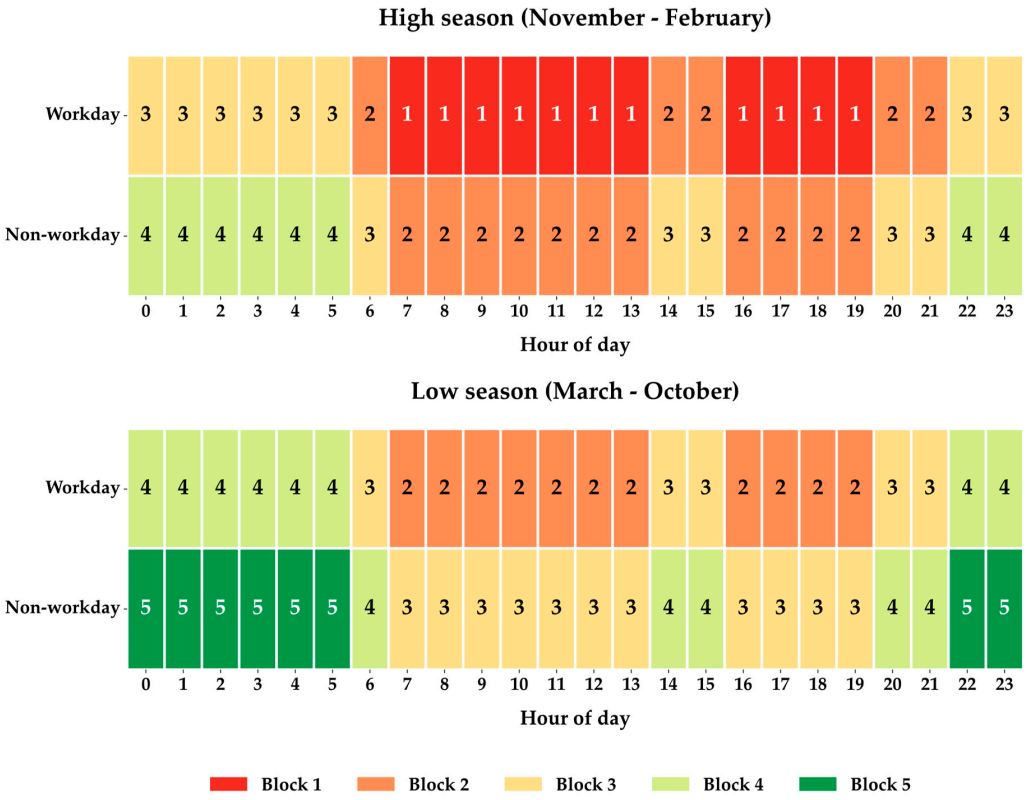

Figure 5. Matrix of tariff time blocks throughout the year and day types in the current Slovenian system.

The most significant cost component is the aggregate capacity tariff c_{cap}. As defined in (7), this fee is disaggregated into several underlying components: $c_{trans,cap}$, $c_{dist,cap}$, and c_{RES}. The specific values for each component, differentiated by season and time block, are detailed in Table 4.

Table 4. Structure of monthly capacity fees by season and time block [35,37,38].

Block	$c_{trans,cap}$ (EUR/kW)		$c_{dist,cap}$ (EUR/kW)		c_{RES} (EUR/kW)		TOTAL c_{cap} (EUR/kW)	
	HS	LS	HS	LS	HS	LS	HS	LS
B1	0.2001	0.1001	3.2224	1.6112	0.7756	0.7756	**4.1981**	**2.4869**
B2	0.0465	0.0465	0.8657	0.8657	0.7756	0.7756	**1.6879**	**1.6879**
B3	0.0091	0.0091	0.1539	0.1539	0.7756	0.7756	**0.9386**	**0.9386**
B4	0.0000	0.0000	0.0041	0.0041	0.7756	0.7756	**0.7797**	**0.7797**
B5	0.0000	0.0000	0.0000	0.0000	0.7756	0.7756	**0.7756**	**0.7756**

In addition to capacity charges, the total variable cost of electricity (c_{vol}) comprises the market energy supply price (c_{market}) and volumetric grid fees. The c_{market} component follows a double-tariff system based on the time schedule defined by the distribution system operator [39]:

- High tariff (HT): 0.1199 EUR/kWh. Active on working days from 06:00 to 22:00.
- Low tariff (LT): 0.0979 EUR/kWh. Active during nighttime hours (22:00–06:00) on working days, and throughout the entire day (00:00–24:00) on non-working days.

The specific market prices used in the simulation are taken from representative retail offers applicable to 2025. Furthermore, the total annual fixed operator fees (C_{fixed}) are calculated as a monthly charge of 1.99 EUR per metering point [40]. Regarding electricity exports, the financial compensation for surplus PV generation injected into the grid (c_{exp}) is set to 0 EUR/kWh, according to [41].

The volumetric network fee consists of transmission ($c_{trans,vol}$) and distribution ($c_{dist,vol}$) fees plus excise duties (c_{tax}). These fees are constant across seasons but vary slightly by time block, as shown in Table 5.

 doi:10.20944/preprints202603.1588.v1

Table 5. Volumetric network fees by time block [35,37].

Block	$c_{\text{trans,vol}}$ (EUR/kWh)	$c_{\text{dist,vol}}$ (EUR/kWh)	c_{tax} (EUR/kWh)	c_{vol} (EUR/kWh)
B1	0.0066	0.0134	0.0015	**0.0215**
B2	0.0059	0.0124	0.0015	**0.0199**
B3	0.0055	0.0126	0.0015	**0.0196**
B4	0.0058	0.0127	0.0015	**0.0201**
B5	0.0059	0.0128	0.0015	**0.0203**

In EC scenarios (scenarios 2, 3, and 4), the model integrates specific economic mechanisms defined by the regulatory framework. The internal market price ($c_{\text{local,market}}$) is calculated using the split-the-difference method defined in equation (10). Based on market prices, $c_{\text{local,market}}$ amounts to 0.0599 EUR/kWh during the HT and 0.0489 EUR/kWh during the LT.

To evaluate potential regulatory incentives, specific exemptions are modeled for ECs. Internally exchanged energy is exempt from the $c_{\text{trans,vol}}$ to reflect reduced grid utilization, while participating prosumers receive a simulated policy exemption from the c_{RES}.

The C-BESS operates as a distinct grid user with its own metering point. Its operational costs are dynamically calculated based on the source of energy:

- Grid import: when charging from the grid, the C-BESS incurs full network charges (c_{cap} and $c_{\text{grid,vol}}$).
- Local charging: when charging from excess community PV generation, it benefits from the same exemptions as P2P exchange.

These operational costs recorded by the C-BESS metering point are distributed among the EC members according to the cost allocation key defined in equation (38).

Crucially, since the C-BESS is an asset owned by the EC, prosumers are exempt from paying the agreed internal market price ($c_{\text{local,market}}$) when discharging the C-BESS. However, regarding network fees, the current regulatory framework results in a "double grid fee" effect: volumetric network charges are paid once by the C-BESS during charging, and effectively paid again by the prosumers when retrieving that energy from the C-BESS.

Regarding the violation of the contracted power (P^h_{con}), a shadow penalty cost (c_{penalty}) is set to 100 EUR/kW. This cost is applied to the excess power variable (P^h_{exc}), defined in equations (31) and (32), to penalize any consumption exceeding the P^h_{con} limits.

The economic assessment relies on a project lifetime (L_{proj}) of 15 years. By applying a discount rate (r) of 3% and an estimated inflation rate of 2.6%, the CRF is calculated according to equation (13), resulting in a value of 0.0838. Furthermore, all end-user financial calculations include a 22% VAT [42].

The BESS CAPEX (c_{BESS}) is set to 500 EUR/kWh for both the centralized and distributed configurations based on [43]. This equalization ensures a fair techno-economic comparison, considering the comparable physical scale of the analyzed systems. To account for battery aging during operation, the specific unit degradation cost (c_{deg}) is set to 0.015 EUR/kWh. In addition to the initial investment, the annual operation and maintenance cost ($C_{\text{O\&M}}$) is set at 5 EUR/kW of the maximum discharging power (P_{dis}) according to [44]. Finally, the decommissioning cost (C_{decomm}) is estimated at 80 EUR/kWh based on [45].

3.2. Scenario Definition and Optimization Settings

This subsection defines the analyzed scenarios and outlines the configuration of the optimization framework. First, it describes the computational hardware, software environment, and the solver applied to execute the optimization. Subsequently, it details the different scenarios formulated for the analysis.

 doi:10.20944/preprints202603.1588.v1

3.2.1. Software Tools and Computational Environment

The proposed optimization model is implemented in Python (version 3.13.9) utilizing the Pyomo modeling framework [46] and solved using the Gurobi Optimizer (version 13.0.0) [47]. As defined in section 2, the simulation process is structured into two sequential phases: the initial co-optimization of the BESS sizing and operation, followed by the operational optimization for the remaining years of the L_{proj}. The time step (Δt) is set to 15 minutes (0.25 hours). All computational tasks were performed on a personal computer running Windows 11 Pro, equipped with an Intel Core i5-14400 processor (2.50 GHz, 10 cores, 16 logical processors) and 32 GB of RAM.

3.2.2. Simulated Scenarios

Six distinct scenarios are defined to evaluate the impact of BESS integration and EC frameworks. These scenarios are structured to compare different investment and operational strategies from the prosumer's perspective. Specifically, they assess the economic viability of operating as an individual prosumer versus participating in an EC, and the financial implications of investing in a centralized BESS versus distributed BESS units. The defined scenarios are:

- Baseline scenario (BS): individual prosumers without BESS
- Baseline EC scenario (BS-EC): EC without BESS
- Scenario 1 (S1): individual prosumers with D-BESS
- Scenario 2 (S2): EC with an optimized C-BESS
- Scenario 3 (S3): EC with a fixed-capacity C-BESS
- Scenario 4 (S4): EC with D-BESS

In the BS, households operate as independent prosumers with PV systems only. They interact directly with the grid without any BESS or P2P trading capabilities, exporting excess generation to the grid. This scenario establishes a benchmark for operation without energy management and serves as the reference case ($C^{h,\text{ref}}_{\text{bill,gross}}$) to calculate the annual net cost savings (ANC^h) achieved through BESS integration strictly for S1. In S1, the optimization model determines the optimal nominal capacity (E^h_{nom}) and operation of a D-BESS for each prosumer, with households still acting outside any community framework.

Conversely, the remaining configurations integrate the prosumers into an EC, enabling internal P2P energy sharing and the application of grid fee exemptions defined in section 3.1.2. To accurately isolate the financial contribution of the BESS from the regulatory benefits of the EC, the BS-EC is introduced. In the BS-EC, prosumers participate in the community with P2P trading but without any BESS installed. This scenario serves as the dedicated reference case ($C^{h,\text{ref}}_{\text{bill,gross}}$) for evaluating ANC^h and the profitability of BESS investments in S2, S3, and S4.

In S2, the optimization model jointly determines the optimal investment and operation of a single C-BESS for the entire community. To provide a direct comparative benchmark, S3 utilizes the identical EC framework, but the C-BESS capacity is not optimized; instead, it is pre-defined and fixed to the exact sum of the optimal individual D-BESS capacities ($\sum_{h=1}^{H} E^h_{\text{nom}}$) obtained in S1. Finally, S4 explores a decentralized community approach in which the optimization model determines the E^h_{nom} and the operation of a D-BESS for each prosumer, similar to S1, but leveraging the financial benefits of P2P trading and the EC regulatory framework

Note that local P2P energy sharing in collaborative EC configurations is modeled as a cooperative pool-based mechanism. For these scenarios, the objective function is formulated to minimize the total aggregated operational cost of the entire EC, rather than simulating competitive bilateral bidding or profit-sharing algorithms among individual peers. While this centralized optimization approach is necessary to determine the absolute techno-economic potential of the integrated BESS capacities, it does not guarantee an equitable distribution of financial savings among individual prosumers. To address this limitation, the fairness of the resulting cost distribution is evaluated ex-post using the Gini coefficient (G). This methodological choice represents a conscious trade-off: it prioritizes evaluating

 doi:10.20944/preprints202603.1588.v1

optimal BESS sizing and operation under capacity-based tariff structures over simulating individual market behaviors, which remains an avenue for future research.

3.3. Optimization Results: BESS Sizing and Investment Costs

The initial stage of the techno-economic assessment determines the optimal BESS capacity and the corresponding C^h_{inv} required to minimize the equivalent annualized TCO. Table 6 summarizes the optimization results for the 15 analyzed prosumers across the evaluated scenarios. For the distributed configurations (S1 and S4), the capacity values represent the directly optimized E^h_{nom}. Conversely, for the centralized EC configurations (S2 and S3), the table presents the $E^h_{\text{bat,alloc}}$, which is determined proportionally to each member's installed PV power according to (39), enabling individual economic evaluation.

Table 6. Optimal BESS capacities and investment costs across scenarios for the base year.

Prosumer ID	Optimal BESS capacity (kWh)				Initial investment cost (EUR)			
	E^h_{nom} S1	$E^h_{\text{bat,alloc}}$ S2	$E^h_{\text{bat,alloc}}$ S3	E^h_{nom} S4	C^h_{inv} S1	C^h_{inv} S2	C^h_{inv} S3	C^h_{inv} S4
H01	3.50	0.00	3.05	0.00	1750.00	0.00	1524.73	0.00
H02	3.50	0.00	5.49	0.00	1750.00	0.00	2744.51	0.00
H03	5.00	0.00	3.05	1.00	2500.00	0.00	1524.73	500.00
H04	1.50	0.00	4.88	0.00	750.00	0.00	2439.56	0.00
H05	3.00	0.00	3.66	1.00	1500.00	0.00	1829.67	500.00
H06	5.00	0.00	4.27	0.00	2500.00	0.00	2134.62	0.00
H07	3.00	0.00	1.83	0.00	1500.00	0.00	914.84	0.00
H08	2.00	0.00	1.83	0.50	1000.00	0.00	914.84	250.00
H09	4.00	0.00	4.88	1.00	2000.00	0.00	2439.56	500.00
H10	5.00	0.00	2.44	1.00	2500.00	0.00	1219.78	500.00
H11	2.00	0.00	3.66	0.00	1000.00	0.00	1829.67	0.00
H12	7.00	0.00	4.88	1.00	3500.00	0.00	2439.56	500.00
H13	5.50	0.00	6.10	0.50	2750.00	0.00	3049.45	250.00
H14	2.50	0.00	1.83	0.00	1250.00	0.00	914.84	0.00
H15	3.00	0.00	3.65	1.00	1500.00	0.00	1829.64	500.00
TOTAL	**55.50**	**0.00**	**55.50**	**7.00**	**27,750.00**	**0.00**	**27,750.00**	**3,500.00**

Optimization results under the Slovenian framework highlight a direct CAPEX-OPEX trade-off. In S1, individual D-BESS investments prove viable, with optimal capacities between 1.5 kWh and 7.0 kWh (totaling 55.5 kWh). By effectively shaving peak loads and reducing contracted power (P^h_{con}) during expensive blocks, OPEX savings exceed annualized CAPEX. As will be detailed in the economic evaluation, this favorable balance is directly reflected in the positive Net Present Value (NPV) outcomes for the prosumers. To benchmark EC operation, S3 adopts this exact 55.5 kWh aggregate capacity and virtually allocates it based on members' PV potential.

Conversely, the optimization model determines an optimal C-BESS capacity of 0 kWh for S2. Because the investment is rejected, the operational and financial outcomes of S2 are functionally identical to the BS-EC scenario, where prosumers generate savings exclusively through P2P energy sharing and regulatory grid fee exemptions without any storage. By minimizing pre-tax annualized costs (C^h_{total}) alongside a cycle penalty (c_{deg}), the MILP objective function evaluates the C-BESS as economically unviable.

This rejection stems from the capacity-based tariff mechanics. Unlike behind-the-meter D-BESS, C-BESS energy must pass through individual smart meters, preventing it from reducing contracted power peaks (P^h_{con}), the primary driver of savings. Moreover, regulatory "double grid fees" on C-BESS operations narrow arbitrage margins, making P2P trading more cost-effective for surplus PV. Since limited operational savings cannot offset CAPEX and degradation, S2's break-even evaluation is deferred to the sensitivity analysis (Section 3.6).

 doi:10.20944/preprints202603.1588.v1

In S4, combining D-BESS with active P2P trading drastically reduces optimal capacities to merely 7.0 kWh total. Profitable P2P conditions prioritize immediate trading of excess PV. The resulting 0.5 to 1.0 kWh micro-capacities represent the mathematical minimum required to shave isolated peaks unresolvable by P2P sharing. Although practically infeasible—as commercial residential units typically exceed 3.0 kWh, this highlights a critical synergy: P2P markets efficiently manage bulk surplus, while D-BESS remains essential for residual peak shaving and securing optimal P^{h}_{con} limits.

3.4. Prosumer-level technical performance and operational savings

To evaluate the technical and economic implications of the optimized configurations, this subsection analyzes the operational dynamics at the individual prosumer level. Presented results refer to the first operative base year ($y = 1$). Since the optimization yielded a 0 kWh BESS capacity for S2, this scenario is excluded from the subsequent detailed technical and economic breakdowns and is evaluated only in the sensitivity analysis in section 3.6. Table 7 presents the monthly breakdown of the gross electricity bill ($C^{h,m}_{\text{bill,gross}}$) for the representative prosumer (H01) across all evaluated scenarios. The sum of these monthly values corresponds to the total annual gross bill ($C^{h}_{\text{bill,gross}}$) calculated using equation (40).

Table 7. Monthly gross electricity bills for prosumer H01 across evaluated scenarios for the base year.

	Monthly gross bill ($C^{h,m}_{\text{bill,gross}}$) (EUR)				
Month	**BS**	**BS-EC**	**S1**	**S3**	**S4**
January	167.77	132.97	136.76	132.58	131.90
February	127.75	93.44	95.18	93.15	92.64
March	88.40	60.53	68.86	58.72	59.36
April	89.13	48.17	61.65	43.51	46.92
May	63.30	34.25	45.34	30.95	33.53
June	45.47	20.55	31.14	14.69	20.12
July	44.60	20.97	32.55	14.00	21.00
August	56.11	28.52	37.74	18.68	27.69
September	73.83	37.20	45.45	30.54	36.37
October	93.24	58.79	68.91	56.32	57.67
November	147.82	103.51	117.01	103.04	102.42
December	219.14	174.23	191.39	174.51	173.35
TOTAL	**1216.56**	**813.13**	**931.98**	**770.64**	**802.97**

The results confirm that all evaluated configurations effectively reduce the prosumer's operational costs compared to the individual baseline (BS). Notably, simply joining the community framework without storage (BS-EC) yields the most substantial initial cost drop, reducing the annual gross bill from 1216.56 EUR to 813.13 EUR purely through P2P energy sharing and regulatory grid fee exemptions.

Integrating BESS provides further targeted operational savings. For the individual prosumer, S1 effectively mitigates costs relative to BS by storing surplus energy and lowering expensive capacity peaks (P^{h}_{con}). Within the EC, S3 and S4 achieve additional cost reductions beyond the BS-EC benchmark, particularly during the summer months when excess solar output is efficiently shifted rather than exported to the grid. While the winter months inherently result in higher bills due to increased heating demand and lower solar generation, the operation of BESS and P2P trading consistently minimizes these seasonal costs across all optimized configurations relative to their respective baselines.

While the monthly financial analysis confirms the economic benefits of EC configurations, a detailed assessment of the contracted power profiles (P^{h}_{con}) reveals differences in how each scenario interacts with the distribution grid. Figure 6 illustrates the optimally contracted power across all 12 months and all 5 specific time blocks for the representative prosumer (H01). The gray cells denote inactive blocks as defined by the Slovenian tariff methodology [35].

 doi:10.20944/preprints202603.1588.v1

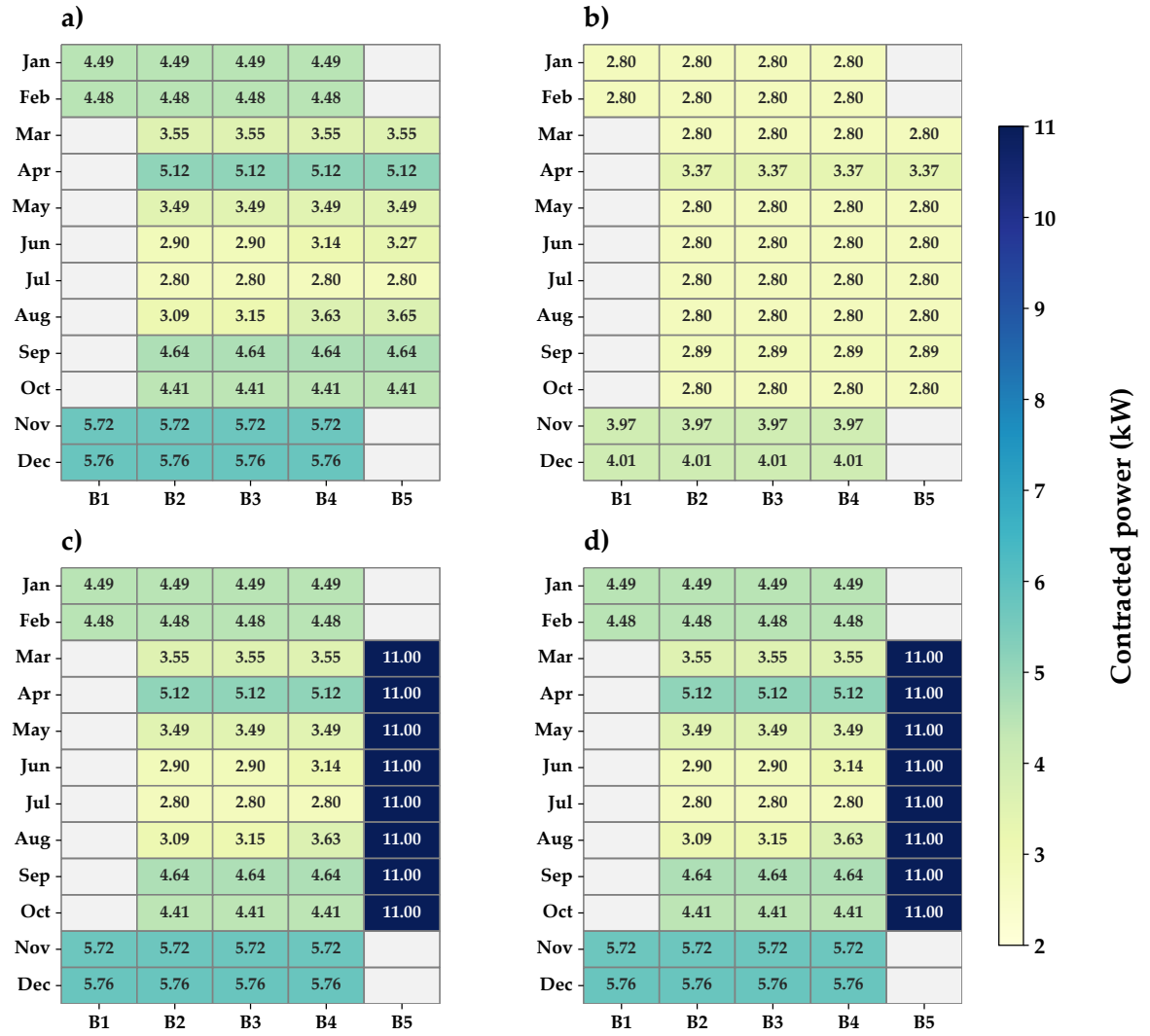

Figure 6. Optimized monthly contracted power by time block for prosumer H01 across evaluated scenarios: (**a**) Baseline; (**b**) Scenario 1; (**c**) Baseline EC and Scenario 3; (**d**) Scenario 4.

The heatmaps clearly show a stark contrast in grid interaction and peak-shaving capabilities among the evaluated configurations. During the winter high season, only the D-BESS in S1 effectively performs behind-the-meter peak shaving. The optimization model reduces the prosumer's physical peak demand in the most expensive block (B1) from 5.76 kW in the BS to 4.01 kW in December, and down to the 2.80 kW technical minimum in January and February, thereby directly minimizing capacity charges.

Conversely, the profiles for S3 and S4 remain identical to the BS-EC benchmark, though for fundamentally different reasons. For S3, this is a systemic limitation: the centralized architecture of the C-BESS cannot physically shave individual meter peaks for any community member. For S4, however, this is a localized economic outcome specific to this representative prosumer, whose optimal D-BESS capacity was 0 kWh; the objective function determined that, given the benefits of P2P trading, paying standard capacity tariffs is more cost-effective for this household than investing in individual storage. Unlike S3, other prosumers in S4 with non-zero D-BESS capacities actively perform peak shaving similar to S1.

A strategic operational shift emerges during the summer low season. While S1 maintains strictly minimized capacity limits across all active blocks, the EC configurations (BS-EC, S3, and S4) intentionally maximize the contracted power in the off-peak block (B5) to the 11.00 kW upper connection limit. Since the capacity fee for B5 is practically zero, the optimization algorithm selects the maximum

 doi:10.20944/preprints202603.1588.v1

limit because it provides absolute operational flexibility at no additional cost. This mathematically optimal choice ensures that the prosumer has the maximum available grid bandwidth for high-volume P2P energy imports and C-BESS discharges without increasing the monthly bill. Consequently, these results demonstrate a fundamental operational trade-off: while D-BESS in S1 minimizes grid reliance to reduce capacity costs, community sharing frameworks strategically leverage free off-peak grid bandwidth to maximize cost-effective energy exchange.

To provide a clear overview of the annual energy balance, Figure 7 presents Sankey diagrams illustrating the energy flows for the representative prosumer (H01) across all evaluated scenarios. These diagrams detail how locally generated PV energy is distributed and how the total household load is met, providing a transparent physical breakdown of energy allocation across each configuration.

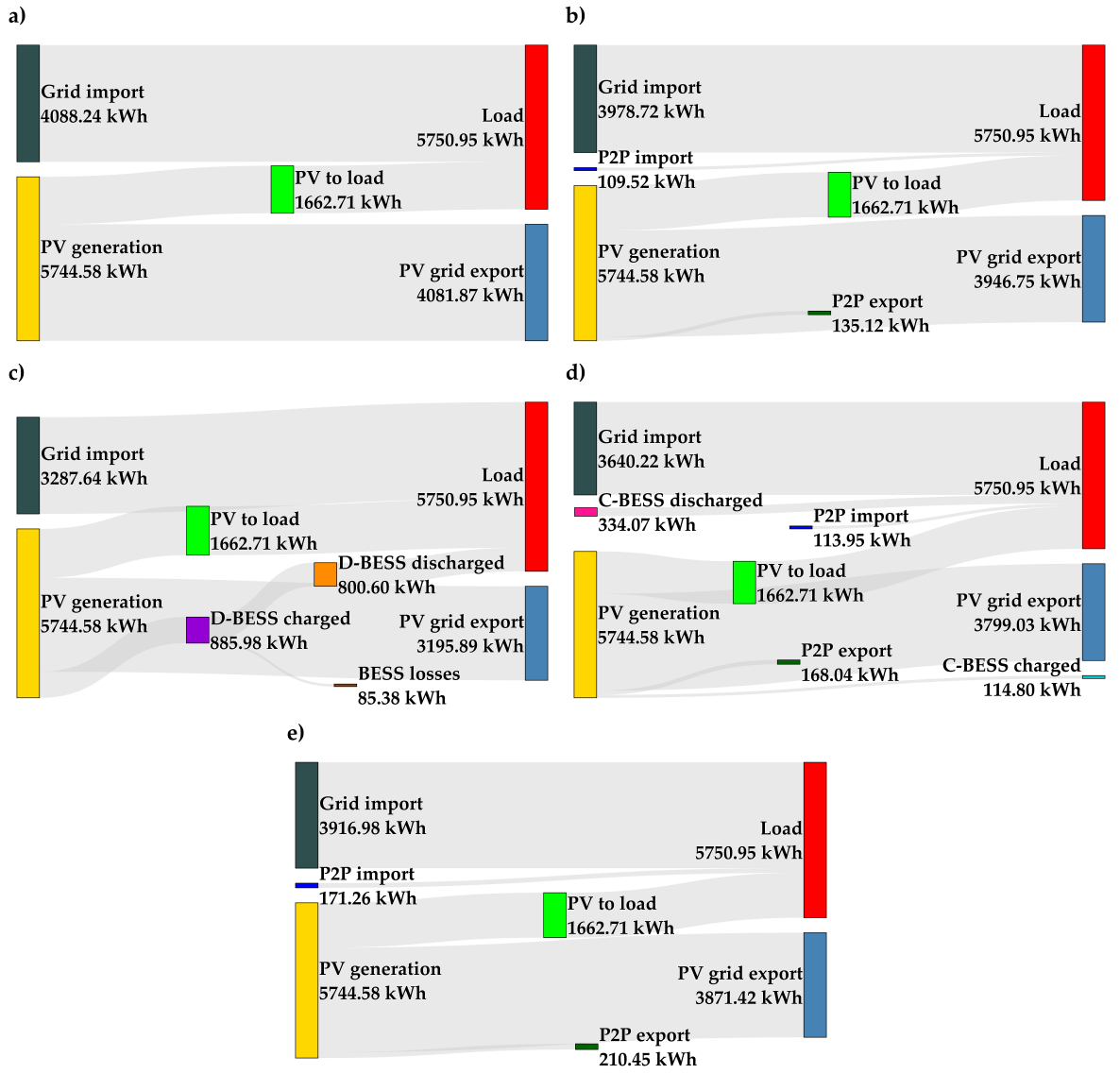

Figure 7. Annual energy flow diagrams (Sankey) for the representative prosumer (H01): (**a**) Baseline; (**b**) Baseline EC; (**c**) Scenario 1; (**d**) Scenario 3; (**e**) Scenario 4.

As illustrated in Figure 7, the BS scenario's PV-load mismatch causes high unremunerated PV to grid export (4081.87 kWh) and significant grid imports. Integrating an individual D-BESS (S1) captures this surplus, minimizing both imports and PV to grid exports, subject only to standard battery conversion losses (85.38 kWh). Conversely, energy flows in the EC scenarios reveal the limitations and dynamics of shared resources. In S3, the C-BESS acts as a shared buffer, with the prosumer

 doi:10.20944/preprints202603.1588.v1

withdrawing more energy (334.07 kWh) than contributed (114.80 kWh), yet failing to meaningfully reduce PV to grid export (3799.03 kWh).

Comparing the BS-EC baseline to S4 highlights the network effects of decentralized storage. In the BS-EC, relying purely on P2P sharing without any community batteries yields only 109.52 kWh of P2P import and 135.12 kWh of P2P export, leaving 3946.75 kWh as unremunerated PV to grid export. In S4, although H01 lacks a D-BESS, the active D-BESS units of other EC members absorb and release energy into the shared pool. This dynamic rerouting increases H01's P2P export to 210.45 kWh and P2P import to 171.26 kWh, directly reducing its grid import to 3916.98 kWh. Consequently, physical energy balances confirm that while individual storage (S1) maximizes direct PV self-consumption, a distributed EC framework (S4) improves energy utilization even for participants without local investments.

Expanding the analysis to all 15 participants, Table 8 details their base-year economic results, presenting final gross electricity bills alongside the absolute and percentage annual net cost savings (*ANC*) calculated via equations (41) and (42). As defined in section 3.2.2, the *ANC* for S1 is benchmarked against the BS scenario, whereas savings for S3 and S4 are calculated relative to the BS-EC scenario. To evaluate individual operational dynamics across scenarios, Table 9 tracks key technical indicators for each prosumer, specifically self-sufficiency ratio (SSR^h), self-consumption ratio (SCR^h), and the power cost share (ξ^h_{power}), derived using equations (34), (35), and (36).

Table 8. Annual gross electricity bills and annual net cost savings for all individual prosumers across the evaluated scenarios during the base year.

Prosumer ID	$C^h_{\text{bill,gross}}$ (EUR)					ANC^h_{abs} (EUR)			ANC^h_{perc} (%)		
	BS	BS-EC	S1	S3	S4	S1	S3	S4	S1	S3	S4
H01	1216.56	813.14	931.98	770.64	802.97	284.58	42.50	10.17	23.39	3.49	0.84
H02	1867.03	1401.30	1576.43	1263.21	1400.32	290.60	138.09	0.98	15.56	7.40	0.05
H03	1241.17	729.49	783.93	692.25	684.29	457.24	37.24	45.20	36.84	3.00	3.64
H04	1312.87	956.26	1211.69	909.34	964.48	101.18	46.92	-8.22	7.71	3.57	-0.63
H05	1140.65	727.00	869.76	671.09	681.24	270.89	55.91	45.76	23.75	4.90	4.01
H06	1601.79	1120.44	1216.69	1057.34	1118.41	385.10	63.10	2.03	24.04	3.94	0.13
H07	1063.23	585.88	846.14	554.26	581.95	217.09	31.62	3.93	20.42	2.97	0.37
H08	820.31	517.82	642.12	463.42	490.56	178.19	54.40	27.26	21.72	6.63	3.32
H09	1496.63	1062.57	1143.79	924.87	1006.80	352.84	137.70	55.77	23.58	9.20	3.73
H10	1046.64	600.76	606.90	509.69	543.34	439.74	91.07	57.42	42.01	8.70	5.49
H11	1104.43	728.74	934.73	635.77	747.76	169.70	92.97	-19.02	15.37	8.42	-1.72
H12	1734.93	1118.68	1112.51	936.54	1061.25	622.42	182.14	57.43	35.88	10.50	3.31
H13	2083.56	1537.20	1624.83	1280.99	1503.38	458.73	256.21	33.82	22.02	12.30	1.62
H14	843.97	529.46	638.66	440.54	523.78	205.31	88.92	5.68	24.33	10.54	0.67
H15	1310.55	894.29	1042.34	699.01	805.45	268.21	195.28	88.84	20.47	14.90	6.78

Table 9. Annual operational metrics for all individual prosumers across the evaluated scenarios.

Prosumer ID	SCR^h (%)					SSR^h (%)					ξ^h_{power} (%)				
	BS	BS-EC	S1	S3	S4	BS	BS-EC	S1	S3	S4	BS	BS-EC	S1	S3	S4
H01	28.94	31.30	44.37	33.87	28.94	28.91	30.82	44.32	36.70	28.91	44.15	18.67	41.03	19.89	18.91
H02	28.31	30.35	37.14	33.11	28.31	27.32	28.26	35.83	38.08	27.32	32.51	11.71	28.52	13.23	11.72
H03	25.59	32.45	49.39	33.85	30.11	28.81	33.05	55.62	40.29	33.38	51.32	23.29	48.30	24.83	22.46
H04	35.92	38.24	40.33	41.99	35.92	37.37	41.77	41.96	45.39	37.37	32.12	11.53	31.43	12.24	11.43
H05	40.19	44.26	52.09	46.21	44.04	42.58	46.33	55.19	54.36	46.24	45.00	19.05	41.94	21.00	17.95
H06	27.53	29.97	41.68	35.94	27.53	26.97	29.19	40.83	34.94	26.97	38.62	14.77	32.80	15.80	14.79
H07	16.42	22.00	29.54	28.69	16.42	17.38	27.12	31.26	33.14	17.38	56.71	28.00	53.30	29.84	28.19
H08	38.00	39.10	53.21	45.11	41.83	34.30	38.87	48.03	49.80	37.40	48.07	20.91	45.84	23.87	20.44
H09	32.23	34.52	44.21	42.91	35.16	33.78	36.19	46.34	48.30	36.54	36.81	13.96	31.69	16.43	13.18
H10	35.83	37.73	62.00	51.92	41.47	36.27	42.70	62.75	58.17	41.38	53.12	23.14	48.18	28.12	22.60
H11	33.05	39.98	41.51	47.12	33.05	35.87	38.93	45.04	52.98	35.87	39.58	15.15	37.95	17.91	14.76
H12	32.55	34.80	51.30	48.66	35.43	33.66	36.88	53.05	53.21	36.33	44.63	17.42	36.32	21.49	16.84
H13	27.54	29.31	39.39	63.12	28.71	27.04	27.90	38.68	45.15	28.08	33.80	11.72	27.11	14.51	11.45
H14	35.10	36.76	53.72	79.01	35.10	32.27	36.84	49.39	55.42	32.27	48.75	21.61	47.12	26.93	21.84
H15	35.43	39.19	46.91	83.18	39.26	33.91	36.33	44.91	59.42	37.21	40.10	15.79	36.02	21.26	15.59

The presented results reveal clear operational distinctions among the evaluated scenarios. When isolating the financial contribution of the shared storage, S3 achieves the highest economic impact among the EC configurations, yielding the maximum ANC^h_{perc} relative to the BS-EC benchmark

 doi:10.20944/preprints202603.1588.v1

(peaking at 14.90% for H15). However, examining the power cost share (ξ^h_{power}) reveals an important mathematical dynamic. Because the centralized architecture in S3 cannot reduce individual contracted power peaks, the absolute capacity costs remain identical to the BS-EC scenario. Consequently, as the C-BESS successfully reduces the volumetric energy costs and lowers the total final bill, these fixed capacity costs inherently represent a slightly larger percentage of the remaining bill.

While the individual approach in S1 delivers the highest absolute financial savings relative to its respective BS benchmark, it is also the superior configuration for maximizing physical self-consumption, consistently achieving the highest SCR^h and SSR^h. Notably, for prosumers where the optimization model allocated zero D-BESS capacity in S4, the physical metrics (SCR^h and SSR^h) and power cost shares (ξ^h_{power}) remain nearly identical to those of the BS-EC.

3.5. Comprehensive Techno-Economic Analysis Results

The long-term economic viability of the proposed configurations was assessed by aggregating financial performance over the 15-year BESS lifetime (L_{proj}), accounting for BESS decommissioning in year 16. Figure 8 illustrates the aggregated cumulative discounted cash flow dynamics for the entire prosumer group across the evaluated scenarios. Complementing this, Table 10 summarizes the final profitability indicators: NPV, ROI, and PBP. These metrics are calculated according to equations (43), (44), and (45). Since the ROI is derived directly from the NPV, any value greater than 0% explicitly indicates pure net profit beyond the recovery of the initial investment. Furthermore, to quantify the fairness of the financial distribution among individual participants, the Gini coefficient (G) is calculated using equation (47).

 doi:10.20944/preprints202603.1588.v1

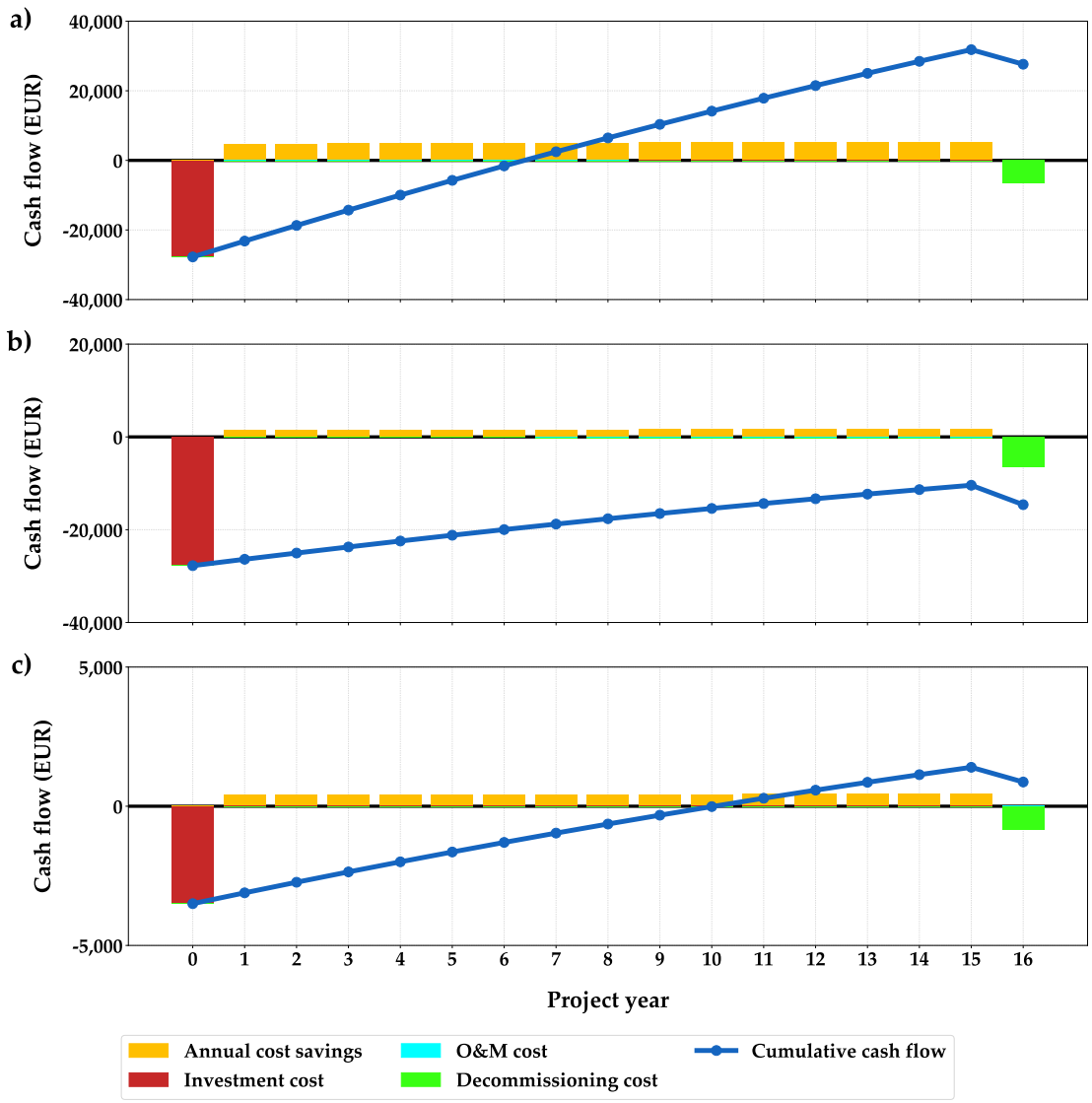

Figure 8. Aggregated cash flow analysis for the evaluated scenarios: (**a**) Scenario 1; (**b**) Scenario 3; and (**c**) Scenario 4.

Table 10. Lifetime economic indicators and Gini coefficients across the evaluated scenarios.

Scenario	C_{inv} (EUR)	*NPV* (EUR)	*ROI* (%)	*PBP* (years)	*G*
S1	27,750.00	27,626.23	99.55	7	0.27
S3	27,750.00	-14,608.16	-52.64	N/A*	0.28
S4	3500.00	870.34	24.87	11	0.25

*Investment not recovered within the project lifetime.

The aggregated results highlight clear differences in investment viability across the operational frameworks. For the individual prosumers (S1), the optimally sized D-BESS achieves strong financial performance, yielding an aggregate *NPV* of 27,626.23 EUR and a *PBP* of 7 years. Conversely, forcing the exact same total battery capacity into a S3 results in a highly negative *NPV* (-14,608.16 EUR) and an unrecoverable investment (*ROI* of -52.64%). This stark financial underperformance definitively justifies the optimization model's decision in S2 to reject the C-BESS investment entirely (0 kWh capacity). As previously established, the C-BESS cannot reduce individual contracted power (P^{h}_{con}) behind the meter and is burdened by double grid fees, rendering it economically unviable.In S4, the optimization model leverages P2P energy trading to satisfy most EC energy-matching needs, drastically reducing D-BESS installations to a total aggregate CAPEX of just 3500 EUR. This minimal investment yields a

 doi:10.20944/preprints202603.1588.v1

positive NPV of 870.34 EUR and an 11-year PBP, confirming the financial viability of the optimized configuration.

These findings provide critical insights into the financial justification of BESS investments within an EC under capacity-based tariffs. While individual D-BESS (S1) is broadly profitable, transitioning to an EC framework shifts the economic focus: unrestricted P2P trading effectively replaces the bulk need for local storage, avoiding substantial CAPEX if internal energy sharing already achieves sufficient savings. Beyond total profitability, the Gini coefficient (G) evaluates the socio-economic fairness of the NPV distribution among the participants, where 0 represents perfect equality and 1 represents absolute inequality. In the individual setup (S1), differences in prosumer load profiles and PV capacities result in a baseline inequality of financial savings ($G = 0.27$). Notably, transitioning to an EC framework does not improve this equity. The G values remain relatively stable, slightly increasing to 0.28 in S3 and marginally decreasing to 0.25 in S4. Although these values indicate a moderately fair distribution of savings overall, the persisting gap confirms a key trade-off: minimizing the total EC costs does not guarantee an equal distribution of the resulting NPV among participants. This highlights the need for dedicated profit-sharing mechanisms in future research.

3.6. Sensitivity Analysis of the Evaluated Scenarios

To evaluate the robustness of the baseline economic findings against future market uncertainties and policy shifts, a sensitivity analysis was conducted across the primary operational frameworks (S1, S3, and S4). This analysis examines the influence of two critical parameters on the aggregated cumulative cash flow. First, the BESS CAPEX (c_{BESS}) was reduced by 40%, from the baseline 500 EUR/kWh to 300 EUR/kWh, to simulate the potential introduction of an incentive framework. Second, the unit volumetric price of electricity imported from the grid ($c_{\text{vol}}(t)$) was increased by 40% to reflect extreme price volatility and inflation in the energy market. Consistent with the defined scenario framework, the fixed C-BESS capacity in S3 dynamically tracks the new optimal aggregate capacities determined in S1 under each evaluated market variation. The impact of these market variations on the cumulative cash flows is illustrated in Figure 9, while the resulting optimal aggregate BESS capacities and final NPV are detailed in Table 11.

Table 11. Aggregate BESS sizing and final NPV under the evaluated market variations.

Market	**S1**		**S3**		**S4**	
condition	$\sum E^{h}_{nom}$ **(kWh)**	NPV **(EUR)**	E^{C-BESS}_{nom} **(kWh)**	NPV **(EUR)**	$\sum E^{h}_{nom}$ **(kWh)**	NPV **(EUR)**
Reference	55.50	27,626.23	55.50	-14,608.16	7.00	870.34
c_{BESS} (-40%)	81.50	44,488.84	81.50	-6599.15	68.00	12,636.24
c_{vol} (+40%)	65.50	41,050.34	65.50	-9005.15	47.50	10,074.00

 doi:10.20944/preprints202603.1588.v1

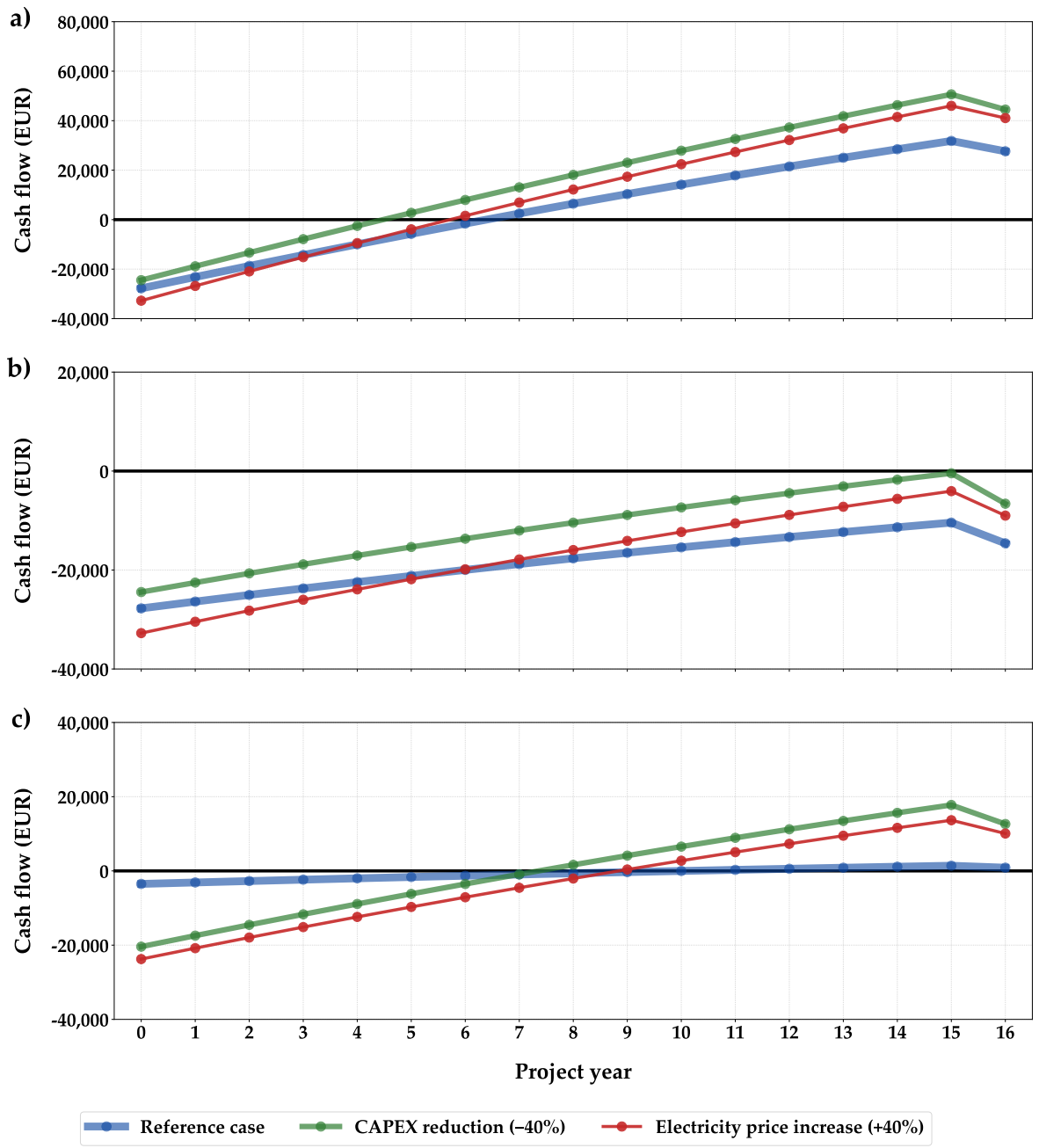

Figure 9. Sensitivity analysis of the cumulative discounted cash flow considering variations in investment costs and electricity prices over the project lifetime for the evaluated scenarios: (**a**) Scenario 1; (**b**) Scenario 3; and (**c**) Scenario 4.

The sensitivity analysis reveals that both market variations significantly affect the optimal BESS sizing and long-term profitability, as detailed in Table 11. In S1, both a 40% reduction in c_{BESS} and a 40% increase in c_{vol} stimulate further investments in D-BESS. The optimal aggregate capacity for the individual prosumers increases from the baseline 55.50 kWh to 81.50 kWh under reduced c_{BESS}, and to 65.50 kWh under elevated c_{vol}. As defined by the scenario framework, the C-BESS capacity in S3 strictly mirrors these capacity expansions. In S1, the CAPEX reduction has a stronger positive impact on the final NPV (44,488.84 EUR) than the c_{vol} increase (41,050.34 EUR), as overcoming the initial investment barrier remains the primary financial bottleneck for individual prosumers. Conversely, in S3, applying these identical capacity expansions results in negative financial outcomes. Even with a 40% reduction in c_{BESS} or a 40% increase in c_{vol}, the NPV remains unrecovered at -6599.15 EUR and -9005.15 EUR, respectively. As illustrated in Figure 9, the annual cash flows in S3 are structurally limited by the

 doi:10.20944/preprints202603.1588.v1

centralized architecture, which cannot perform individual behind-the-meter peak shaving under the capacity-based tariff. Consequently, maintaining the exact aggregate capacity of S1 within a centralized community setup proves economically unviable across all evaluated market conditions.

The most profound change in system behavior is observed in S4. In the reference setup, unrestricted P2P trading provided a cheaper mechanism for minimizing EC costs compared to investing in storage, resulting in a minimal aggregate capacity ($\sum E^{h}_{\text{nom}}$) of 7.00 kWh. However, the sensitivity analysis shows that altering the market parameters substantially alters the investment logic. When c_{BESS} decreases by 40%, the optimization model increases the total $\sum E^{h}_{\text{nom}}$ to 68.00 kWh. Similarly, under a 40% increase in c_{vol}, the EC invests in 47.50 kWh of BESS capacity to minimize expensive grid imports. Consequently, these variations push the final NPV in S4 to 12,636.24 EUR and 10,074.00 EUR, respectively. This proves that lower BESS costs or higher electricity prices stimulate the parallel utilization of local energy sharing and battery storage. Under these modified conditions, S4 significantly outperforms the centralized S3 configuration. It ensures community-wide profitability while equipping prosumers with their own D-BESS units, which effectively reduces individual peak consumption and creates a mutually beneficial setup for the prosumers, the EC, and the distribution grid.

To determine the exact CAPEX at which the optimization algorithm integrates a C-BESS, a break-even analysis was conducted within S2. The analysis reveals that a 55% reduction, lowering c_{BESS} to 225 EUR/kWh, acts as the critical break-even point. At this price level, the model allocates an optimal C-BESS capacity of 26.50 kWh ($E^{\text{C-BESS}}_{\text{nom}}$), resulting in an aggregate investment of 5962.50 EUR. Consequently, this configuration achieves a positive final NPV of 920.60 EUR, an ROI of 15.44%, and a PBP of 10 years.

4. Discussion

The outcomes confirm that under this framework, profitability is not primarily driven by energy arbitrage, but by actively minimizing contracted power (P_{con}) during peak winter blocks. In the case of individual prosumers with D-BESS (S1), distributed units successfully executed behind-the-meter peak shaving, directly lowering individual capacity charges. However, an operational limitation emerges in community-based setups. As demonstrated by the negative financial outcomes of the EC with a fixed-capacity C-BESS (S3), the C-BESS physically cannot reduce individual P_{con} limits. Because energy discharged from the C-BESS to a household passes through the prosumer's primary meter, it is registered as standard grid import subject to volumetric and capacity tracking. Consequently, while centralized storage aggregates community loads and reduces volumetric energy costs, it lacks the direct behind-the-meter peak shaving capability of D-BESS, ultimately rendering it economically unviable under the current capacity-based tariff.

This inability to reduce individual capacity limits is further complicated by the current grid fee structure, which directly dictates optimal BESS sizing. When evaluating the central battery under baseline market conditions (S2), the optimization model allocated exactly 0 kWh of capacity. The primary cause for this rejection is the so-called "double grid fee" mechanism: the C-BESS is treated as an independent grid user. Deprived of capacity-based savings, its financial justification within the solver relies solely on energy arbitrage. However, the double grid fees reduce this arbitrage margin, making it impossible to cover the annualized capital costs and the cycle degradation penalty (c_{deg}). To evaluate the operational potential of centralized storage despite this solver rejection, S3 was established by pre-defining the C-BESS capacity to 55.50 kWh, matching the exact sum of the individual capacities obtained in S1. Although operating this fixed capacity smooths the aggregate energy exchange with the main grid, it does not translate to proportional financial benefits for the prosumers. In fact, comparing S3 to the BS-EC benchmark reveals that the C-BESS actually increases the relative power cost share (ξ_{power}). Because the absolute capacity costs remain fixed while volumetric energy costs decrease, the capacity fee mathematically becomes a larger fraction of the final bill. These findings validate the theoretical models presented in [23] and [25], which demonstrate that shared infrastructure offers

 doi:10.20944/preprints202603.1588.v1

superior aggregate load smoothing. Simultaneously, the complete investment rejection in S2, alongside the negative financial returns in S3, confirms the conclusions of [31] and [32], emphasizing that local tariff rules and grid fees ultimately dictate the practical feasibility of these models.

The comprehensive techno-economic indicators confirm that capacity-based network tariffs significantly enhance the investment potential of BESS. While individual prosumers with D-BESS (S1) maximize the self-consumption ratio (SCR) and self-sufficiency ratio (SSR) and achieve strong absolute profitability, evaluating distributed storage within an active P2P framework (S4) reveals a highly efficient alternative operational strategy. Since P2P trading efficiently manages the EC's PV surplus, the optimization model minimizes the required physical D-BESS capacity. In this setup, P2P trading handles the bulk of energy sharing among participants, while targeted D-BESS units are deployed strictly for peak shaving. This operational strategy yields a positive NPV of 870.34 EUR and an ROI of 24.87%. This mechanism confirms the findings of [27] and [28], which concluded that P2P platforms allow prosumers to effectively exchange excess generation and significantly reduce payback periods. Beyond overall profitability, the Gini coefficient (G) analysis reveals critical insights into the socio-economic sphere. While community integration is often expected to act as an equalizing mechanism, transitioning from isolated operation (S1, $G = 0.27$) to collaborative frameworks does not significantly reduce financial inequality among participants. The G values remain relatively stable, slightly increasing to 0.28 in S3 and marginally decreasing to 0.25 in S4. This highlights a fundamental trade-off: minimizing the total EC costs mathematically ensures collective efficiency, but it does not guarantee a just distribution of the generated savings. Furthermore, the sensitivity analysis confirms the robustness of these configurations against market volatility. A simulated reduction in BESS CAPEX (c_{BESS}) or an increase in volumetric cost for energy import (c_{vol}) stimulates investments in larger battery capacities across the distributed setups (S1 and S4). Specifically, the break-even analysis for the EC with an optimized C-BESS (S2) reveals that a 55% decline in capital costs, lowering c_{BESS} to 225 EUR/kWh, is required for the optimization model to allocate a modestly sized C-BESS capacity under strict baseline market rules. This confirms that anticipated future cost reductions will effectively bridge the gap between theoretical centralized EC benefits and practical investment viability.

The insights derived from this techno-economic analysis provide a solid foundation for several future research directions. First, future work should expand the current energy storage model by incorporating combined cyclic and calendar aging mechanisms, along with variable charge and discharge efficiencies, to enable a more precise economic assessment of lifetime. Additionally, the present deterministic approach relies on perfect foresight for PV generation and load profiles. Integrating stochastic or robust optimization methods would effectively account for these real-world forecasting uncertainties. Within the market framework, the local energy-sharing model could be evolved from a centralized community pool to a fully decentralized bilateral P2P trading mechanism to evaluate individual prosumer negotiation strategies. Moreover, developing dedicated profit-sharing mechanisms or fairness-oriented objective functions is essential to address the socio-economic inequalities highlighted by the Gini coefficient analysis. Furthermore, exploring alternative business models for centralized storage, such as cloud energy storage systems, where participants pay a service fee for virtual capacity, represents a promising alternative to direct EC ownership. Expanding the operational scope to encompass multiple interacting ECs could also unlock new revenue streams by providing ancillary services to the distribution system operator. Finally, integrating detailed technical network constraints, specifically active voltage regulation, into the optimization framework remains a critical future goal to ensure that the maximized economic benefits of ECs do not lead to voltage violations within the local grid.

5. Conclusions

In this paper, a techno-economic framework was developed to evaluate the integration of BESS under an emerging capacity-based tariff structure, specifically analyzed through the Slovenian regulatory context. A MILP optimization model was utilized to co-optimize BESS sizing and operation

 doi:10.20944/preprints202603.1588.v1

during the first year. For the remainder of the project lifetime, the model systematically reduces the battery's SOH and optimizes its operation based on this degraded capacity. Consequently, the study confirmed that BESS investments are highly profitable for distributed architectures (D-BESS), whereas centralized community storage (C-BESS) faces critical economic barriers under the current regulatory conditions. The results demonstrate that under multi-block capacity charges, storage systems are utilized not merely for traditional energy arbitrage, but primarily for active peak shaving.

The comparative analysis revealed clear financial distinctions between storage architectures. While individual D-BESS units yield strong positive returns, centralized storage financially underperforms, resulting in a negative NPV due to its inability to reduce individual capacity peaks. Furthermore, integrating D-BESS within an EC framework minimizes the required physical capacity, yielding a realistic ROI of 24.87%. The evaluation also revealed that ECs do not automatically serve as socio-economic equalizers; the Gini coefficient remained relatively stable, demonstrating that community-wide cost minimization does not guarantee an equitable distribution of financial savings among prosumers.

Finally, the sensitivity analysis demonstrated how the evaluated configurations respond to market volatility. While C-BESS theoretically offers substantial advantages, including economies of scale, enhanced community load smoothing, and increased operational flexibility, the current regulatory conditions severely limit its financial viability. Specifically, the application of double grid fees and the inability to reduce individual contracted power prevent the profitable operation of this shared asset. The break-even analysis revealed that a minimum 55% reduction in capital costs is required for the optimization model to allocate C-BESS capacity. Consequently, under the existing capacity-based tariff framework, the economic deployment of ECs is currently most effectively realized through D-BESS rather than C-BESS.

Author Contributions: Conceptualization, D.Š. and D.T.; methodology, T.M.,M.Ž.,D.Š.,E.L. and D.T.; software, T.M. and M.Ž.; formal analysis, T.M.; investigation, T.M.; data curation, M.Ž.,D.Š.,E.L. and D.T.; writing—original draft preparation, T.M.; writing—review and editing, M.Ž.,D.Š.,E.L. and D.T.; visualization, T.M. and M.Ž.; supervision, M.Ž.,D.Š. and D.T.; All authors have read and agreed to the published version of the manuscript.

Funding: This research received no external funding.

Institutional Review Board Statement: Not applicable.

Informed Consent Statement: Not applicable.

Data Availability Statement: The data presented in this study are available on request from the corresponding author. The data are not publicly available due to privacy.

Acknowledgments: The research presented in this paper and the work of Tomislav Markotić were supported by the Croatian Science Foundation under the "Young researchers' career development project – training of doctoral students" (grant number DOK-2025-02-8476). Furthermore, this work was partially supported by the European Union's Horizon Europe Framework Programme: HORIZON-WIDERA-2023-ACCESS-04, Pathways to Synergies—Coordination and Support Actions—under the project name SynGRID—Creating synergies in Widening countries on the topic of low-voltage grid management (grant number 101160145).

Conflicts of Interest: The authors declare no conflicts of interest.

References

1. International Energy Agency (IEA). Electricity Grids and Secure Energy Transitions. IEA: Paris, France, 2023. Available online: https://www.iea.org/reports/electricity-grids-and-secure-energy-transitions (accessed on 9 February 2026).
2. European Commission. REPowerEU. European Commission: Brussels, Belgium, 2022. Available online: https://commission.europa.eu/topics/energy/repowereu_en (accessed on 9 February 2026).
3. Dubravac, M.; Žnidarec, M.; Fekete, K.; Topić, D. Multi-Stage Operation Optimization of PV-Rich Low-Voltage Distribution Networks. *Applied Sciences* **2024**, *14*. https://doi.org/10.3390/app14010050.

 doi:10.20944/preprints202603.1588.v1

4. Ejuh Che, E.; Roland Abeng, K.; Iweh, C.D.; Tsekouras, G.J.; Fopah-Lele, A. The Impact of Integrating Variable Renewable Energy Sources into Grid-Connected Power Systems: Challenges, Mitigation Strategies, and Prospects. *Energies* **2025**, *18*. https://doi.org/10.3390/en18030689.
5. Majeed, I.B.; Nwulu, N.I. Reverse Power Flow Due to Solar Photovoltaic in the Low Voltage Network. *IEEE Access* **2023**, *11*, 44741–44758. https://doi.org/10.1109/ACCESS.2023.3273483.
6. Aziz, T.; Ketjoy, N. PV Penetration Limits in Low Voltage Networks and Voltage Variations. *IEEE Access* **2017**, *5*, 16784–16792. https://doi.org/10.1109/ACCESS.2017.2747086.
7. Alonso, A.M.S.; Marafão, F.P.; Tedeschi, E. Dispatchable Microgrids: An Extended Provision of Systemic Ancillary Services to Low-Voltage Distribution Grids. *IEEE Access* **2024**, *12*, 76692–76706. https://doi.org/10.1109/ACCESS.2024.3406899.
8. Šljivac, D.; Nakomčić-Smaragdakis, B.; Vukobratović, M.; Topić, D.; Čepić, Z. Cost-benefit comparison of on-grid photovoltaic systems in Pannonian parts of Croatia and Serbia. *Tehnički vjesnik* **2014**, *21*, 1149–1157. Available online: https://hrcak.srce.hr/129131.
9. Nyamathulla, S.; Dhanamjayulu, C. A review of battery energy storage systems and advanced battery management system for different applications: Challenges and recommendations. *Journal of Energy Storage* **2024**, *86*, 111179. https://doi.org/https://doi.org/10.1016/j.est.2024.111179.
10. Žnidarec, M.; Šljivac, D.; Knežević, G.; Pandžić, H. Double-layer microgrid energy management system for strategic short-term operation scheduling. *International Journal of Electrical Power & Energy Systems* **2024**, *157*, 109816. https://doi.org/https://doi.org/10.1016/j.ijepes.2024.109816.
11. Thirunavukkarasu, G.S.; Seyedmahmoudian, M.; Jamei, E.; Horan, B.; Mekhilef, S.; Stojcevski, A. Role of optimization techniques in microgrid energy management systems—A review. *Energy Strategy Reviews* **2022**, *43*, 100899. https://doi.org/https://doi.org/10.1016/j.esr.2022.100899.
12. Markotić, T.; Šljivac, D.; Marić, P.; Žnidarec, M. Sustainable Integration of Prosumers' Battery Energy Storage Systems' Optimal Operation with Reduction in Grid Losses. *Sustainability* **2025**, *17*. https://doi.org/10.3390/su17157165.
13. Dias de Lima, T.; Faria, P.; Vale, Z. Optimizing home energy management systems: A mixed integer linear programming model considering battery cycle degradation. *Energy and Buildings* **2025**, *329*, 115251. https://doi.org/https://doi.org/10.1016/j.enbuild.2024.115251.
14. Ren, Z.; Chen, X.; Dong, Y. Two-stage optimization of appliance scheduling and BESS capacity with comfort level. *Electric Power Systems Research* **2026**, *255*, 112771. https://doi.org/https://doi.org/10.1016/j.epsr.2026.112771.
15. Mohamed, A.A.; Best, R.J.; Liu, X.; Morrow, D.J. A Comprehensive Robust Techno-Economic Analysis and Sizing Tool for the Small-Scale PV and BESS. *IEEE Transactions on Energy Conversion* **2022**, *37*, 560–572. https://doi.org/10.1109/TEC.2021.3107103.
16. Alic, A.; Spada, A.; Zordan, S.; De Paola, A.; Trovato, V. Optimal operation and revamping of a battery storage integrated with photovoltaic in renewable energy communities: A dynamic programming approach. *Sustainable Energy, Grids and Networks* **2025**, *44*, 101976. https://doi.org/https://doi.org/10.1016/j.segan.2025.101976.
17. Pigem, J.M.; García-Muñoz, F.; Bravo, N.J.; Aránguiz, R.; Burgos, V.C. Optimal sizing of community photovoltaic and battery energy storage systems with second-life batteries in peer-to-peer energy communities. *Journal of Energy Storage* **2026**, *148*, 120031. https://doi.org/https://doi.org/10.1016/j.est.2025.120031.
18. Chreim, B.; Esseghir, M.; Merghem-Boulahia, L. Recent sizing, placement, and management techniques for individual and shared battery energy storage systems in residential areas: A review. *Energy Reports* **2024**, *11*, 250–260. https://doi.org/https://doi.org/10.1016/j.egyr.2023.11.053.
19. Zhou, Y. Renewable-storage sizing approaches for centralized and distributed renewable energy—A state-of-the-art review. *Journal of Energy Storage* **2024**, *100*, 113688. https://doi.org/https://doi.org/10.1016/j.est.2024.113688.
20. Korjani, S.; Casu, F.; Damiano, A.; Pilloni, V.; Serpi, A. An online energy management tool for sizing integrated PV-BESS systems for residential prosumers. *Applied Energy* **2022**, *313*, 118765. https://doi.org/https://doi.org/10.1016/j.apenergy.2022.118765.
21. Fernandez, E.; Hossain, M.; Nawazish Ali, S.; Sharma, V. An efficient P2P energy trading platform based on evolutionary games for prosumers in a community. *Sustainable Energy, Grids and Networks* **2023**, *34*, 101074. https://doi.org/https://doi.org/10.1016/j.segan.2023.101074.

 doi:10.20944/preprints202603.1588.v1

22. Li, P.; Chen, J.; Yang, H.; Lin, Z. Peer-to-peer power trading and pricing for rental energy storage shared community microgrid: A coordinated Stackelberg and cooperative game. *Renewable Energy* **2026**, *256*, 123963. https://doi.org/https://doi.org/10.1016/j.renene.2025.123963.
23. Guo, F.; Gomes, L.; Ma, L.; Tian, Z.; Vale, Z.; Pang, S. Optimizing battery storage for sustainable energy communities: A multi-scenario analysis. *Sustainable Cities and Society* **2025**, *118*, 106030. https://doi.org/https://doi.org/10.1016/j.scs.2024.106030.
24. Domenech, C.B.; De Corato, A.M.; Mancarella, P. Co-Optimization of Behind-the-Meter and Front-of-Meter Value Streams in Community Batteries. *Journal of Modern Power Systems and Clean Energy* **2024**, *12*, 334–345. https://doi.org/10.35833/MPCE.2023.000746.
25. Rodrigues, D.L.; Ye, X.; Xia, X.; Zhu, B. Battery energy storage sizing optimisation for different ownership structures in a peer-to-peer energy sharing community. *Applied Energy* **2020**, *262*, 114498. https://doi.org/https://doi.org/10.1016/j.apenergy.2020.114498.
26. Zakeri, B.; Gissey, G.C.; Dodds, P.E.; Subkhankulova, D. Centralized vs. distributed energy storage – Benefits for residential users. *Energy* **2021**, *236*, 121443. https://doi.org/https://doi.org/10.1016/j.energy.2021.121443.
27. Zheng Wang.; Luther, M.; Horan, P.; Matthews, J.; Liu, C. Technical and economic analyses of grid-connected residential PV considering batteries and peer-to-peer energy sharing. *Renewable Energy* **2025**, *252*, 123494. https://doi.org/https://doi.org/10.1016/j.renene.2025.123494.
28. Ali, L.; Azim, M.I.; Peters, J.; Pashajavid, E. Expediting battery investment returns for residential customers utilising spot price-aware local energy exchanges. *Energy* **2024**, *306*, 132458. https://doi.org/https://doi.org/10.1016/j.energy.2024.132458.
29. Bahramara, S.; Khezri, R.; Haque, M.H. Resiliency-Oriented Economic Sizing of Battery for a Residential Community: Cloud Versus Distributed Energy Storage Systems. *IEEE Transactions on Industry Applications* **2024**, *60*, 1963–1974. https://doi.org/10.1109/TIA.2023.3311774.
30. Pocola, T.O.; Robu, V.; Rietveld, J.; Norbu, S.; Couraud, B.; Andoni, M.; Flynn, D.; Poor, H. Optimal sizing and control of a grid-connected battery in a stacked revenue model including an energy community. *Applied Energy* **2025**, *397*, 126122. https://doi.org/https://doi.org/10.1016/j.apenergy.2025.126122.
31. Casella, V.; Ferro, G.; Parodi, L.; Robba, M. Maximizing shared benefits in renewable energy communities: A Bilevel optimization model. *Applied Energy* **2025**, *386*, 125562. https://doi.org/https://doi.org/10.1016/j.apenergy.2025.125562.
32. Barchi, G.; Pierro, M.; Secchi, M.; Moser, D. Fully Solar Residential Energy Community: A Study on the Feasibility in the Italian Context. *Energies* **2025**, *18*. https://doi.org/10.3390/en18081988.
33. European Commission, Joint Research Centre. Photovoltaic Geographical Information System (PVGIS) version 5.3. European Commission: Ispra, Italy, 2025. Available online: https://joint-research-centre.ec.europa.eu/pvgis-photovoltaic-geographical-information-system_en (accessed on 28 January 2026).
34. SODO d.o.o.. Cenik omrežnine za priključno moč za leto 2025 [Network Tariff Price List for Contracted Capacity for the Year 2025]. SODO d.o.o.: Maribor, Slovenia, 2025. (In Slovenian). Available online: https://sodo.si/storage/app/uploads/public/673/ed0/8a5/673ed08a55566141828123.pdf (accessed on 17 February 2026).
35. Agencija za energijo. Akt o metodologiji za obračunavanje omrežnine za elektrooperaterje (neuradno prečiščeno besedilo št. 10) [Act on the Methodology for Charging the Network Charge for Electricity Operators (unofficial consolidated text No. 10)]. Agencija za energijo: Maribor, Slovenia, 2025. (In Slovenian). Available online: https://pisrs.si/pregledPredpisa?id=AKT_1266 (accessed on 11 February 2026).
36. Agencija za energijo. Tarifne postavke omrežnine za leto 2025 [Network Tariff Rates for the Year 2025]. Agencija za energijo: Maribor, Slovenia, 2025. (In Slovenian). Available online: https://www.agen-rs.si/documents/10926/35701/Tarifne-postavke-omreznine-za-leto-2025/304dc3b0-f00a-4a0f-8f41-6e86418655c2 (accessed on 17 February 2026).
37. Agencija za energijo. Akt o določitvi tarifnih postavk za omrežnine elektrooperaterjev (neuradno prečiščeno besedilo št. 1) [Act on Determining Tariff Rates for Electricity Operators' Network Charges (unofficial consolidated text No. 1)]. Official Gazette of the Republic of Slovenia: Ljubljana, Slovenia, 2025. (In Slovenian). Available online: https://pisrs.si/pregledPredpisa?id=ANJP82 (accessed on 17 February 2026).
38. Agencija za energijo. Akt o prispevkih za zagotavljanje podpor za proizvodnjo električne energije iz obnovljivih virov energije in v soproizvodnji z visokim izkoristkom [Act on contributions to ensure support for the production of electricity from renewable energy sources and in high-efficiency cogeneration]. Official

 doi:10.20944/preprints202603.1588.v1

Gazette of the Republic of Slovenia, No. 83/24, 14/25, 84/25 and 112/25: Ljubljana, Slovenia, 2024. (In Slovenian). Available online: https://pisrs.si/pregledPredpisa?id=ANJP25 (accessed on 24 February 2026).
39. SODO d.o.o.. Meritve [Measurements – FAQ]. SODO d.o.o.: Maribor, Slovenia, 2026. (In Slovenian). Available online: https://www.sodo.si/pogosta-vprasanja/meritve (accessed on 18 February 2026).
40. GEN-I d.o.o.. Redni cenik električne energije za gospodinjske odjemalce [Regular Price List for Electricity for Household Customers]. GEN-I d.o.o.: Ljubljana, Slovenia, 2026. (In Slovenian). Available online: https://gen-i.si/en/households/electricity/pricelists-and-special-offers/redni-cenik-elektricne-energije-za-gospodinjske-odjemalce/ (accessed on 18 February 2026).
41. Državni zbor Republike Slovenije. Zakon o spodbujanju rabe obnovljivih virov energije (ZSROVE) (neuradno prečiščeno besedilo št. 3) [Act on the Promotion of the Use of Renewable Energy Sources (unofficial consolidated text No. 3)]. Official Gazette of the Republic of Slovenia: Ljubljana, Slovenia, 2025. (In Slovenian). Uradni list RS, št. 121/21, 189/21, 121/22, 102/24 in 112/25. Available online: https://pisrs.si/pregledPredpisa?id=ZAKO8236 (accessed on 17 February 2026).
42. Republic of Slovenia. Zakon o davku na dodano vrednost (ZDDV-1) [Value Added Tax Act]. Official Gazette of the Republic of Slovenia, No. 13/11, 122/23, 104/24, 2024. (In Slovenian). Available online: https://pisrs.si/pregledPredpisa?id=ZAKO4701 (accessed on 19 February 2026).
43. SolarPower Europe. European Market Outlook for Battery Storage 2025–2029, 2025. Available online: https://www.solarpowereurope.org (accessed on 19 February 2026).
44. EPRI. Battery Energy Storage Lifecycle Cost Assessment Summary. EPRI: Palo Alto, CA, USA, 2020. Available online: https://www.epri.com/research/programs/053125/results/3002020048 (accessed on 19 February 2026).
45. EPRI. Recycling and Disposal of Battery-Based Grid Energy Storage Systems: A Preliminary Investigation. EPRI: Palo Alto, CA, USA, 2017. Available online: https://www.epri.com/research/products/000000003002006911 (accessed on 19 February 2026).
46. Hart, W.E.; Watson, J.P.; Woodruff, D.L. Pyomo: Modeling and Solving Mathematical Programs in Python. *Mathematical Programming Computation* **2011**, *3*, 219–260. https://doi.org/10.1007/s12532-011-0026-8.
47. Gurobi Optimization, LLC. Gurobi Optimizer Reference Manual. Gurobi Optimization, LLC: Beaverton, OR, USA, 2026. Version 13.0.0. Available online: https://docs.gurobi.com/projects/optimizer/en/current/ (accessed on 19 February 2026).